Neural Networks 153 (2022) 496–517

Contents lists available at ScienceDirect

Neural Networks

journal homepage: www.elsevier.com/locate/neunet

Oblique and rotation double random forest

M.A. Ganaie [a], M. Tanveer [a,*], P.N. Suganthan [b,c,*], V. Snasel [d]

[a] Department of Mathematics, Indian Institute of Technology Indore, Simrol, Indore, 453552, India
[b] School of Electrical & Electronic Engineering, Nanyang Technological University, Singapore
[c] KINDI Center for Computing Research, College of Engineering, Qatar University, Qatar
[d] Department of Computer Science, VŠB - Technical University of Ostrava, Czech Republic

ARTICLE INFO

Article history:
Received 5 November 2021
Received in revised form 25 May 2022
Accepted 9 June 2022
Available online 18 June 2022

Keywords:
Double random forest
Oblique random forest
Ensemble learning
Bootstrap
Decision tree
classification

ABSTRACT

Random Forest is an ensemble of decision trees based on the bagging and random subspace concepts. As suggested by Breiman, the strength of unstable learners and the diversity among them are the ensemble models' core strength. In this paper, we propose two approaches known as oblique and rotation double random forests. In the first approach, we propose rotation based double random forest. In rotation based double random forests, transformation or rotation of the feature space is generated at each node. At each node different random feature subspace is chosen for evaluation, hence the transformation at each node is different. Different transformations result in better diversity among the base learners and hence, better generalization performance. With the double random forest as base learner, the data at each node is transformed via two different transformations namely, principal component analysis and linear discriminant analysis. In the second approach, we propose oblique double random forest. Decision trees in random forest and double random forest are univariate, and this results in the generation of axis parallel split which fails to capture the geometric structure of the data. Also, the standard random forest may not grow sufficiently large decision trees resulting in suboptimal performance. To capture the geometric properties and to grow the decision trees of sufficient depth, we propose oblique double random forest. The oblique double random forest models are multivariate decision trees. At each non-leaf node, multisurface proximal support vector machine generates the optimal plane for better generalization performance. Also, different regularization techniques (Tikhonov regularization, axis-parallel split regularization, Null space regularization) are employed for tackling the small sample size problems in the decision trees of oblique double random forest. The proposed ensembles of decision trees produce trees with bigger size compared to the standard ensembles of decision trees as bagging is used at each non-leaf node which results in improved performance. The evaluation of the baseline models and the proposed oblique and rotation double random forest models is performed on benchmark 121 UCI datasets and real-world fisheries datasets. Both statistical analysis and the experimental results demonstrate the efficacy of the proposed oblique and rotation double random forest models compared to the baseline models on the benchmark datasets.

1. Introduction

Perturb and combine approach (Breiman, 1996a) is the core of the ensemble strategy (Dietterich, 2000) and hence, it has been used across different domains like machine learning (Wiering & Van Hasselt, 2008), computer vision tasks (Goerss, 2000) for recognition of patterns, mining big data (Lulli, Oneto, & Anguita, 2019) and biomedical domain (Pal & Parija, 2021). Both theoretical and empirical aspects of the ensemble learning have been explored in the literature. Multiple classifier systems (Zhou, Roli, Kittler, et al., 2013) or ensemble learning perturbs the input data to induce diversity among the base learners of an ensemble and uses combine strategy to aggregate the outputs of base learners such that the generalization of the ensemble model is superior in comparison with the individual learners.

To analyze how the ensemble learning performs better compared to individual models, studies like reduction in variance among the base learners (Breiman, 1996a; Geurts, Ernst, & Wehenkel, 2006; Zhang & Zhang, 2008) have been put forth. With the bias and variance reduction theory (Breiman, 1996a; Kohavi, Wolpert, et al., 1996), the error in classification is given in terms of bias and variance. Bias measure gives how far is the average guess of each base learner from the target class over the

* Corresponding authors.
E-mail addresses: phd1901141006@iiti.ac.in (M.A. Ganaie), mtanveer@iiti.ac.in (M. Tanveer), epnsugan@ntu.edu.sg (P.N. Suganthan), vaclav.snasel@vsb.cz (V. Snasel).

https://doi.org/10.1016/j.neunet.2022.06.012
0893-6080/

Nomenclature

PCA	Principal component analysis
LDA	Linear discriminant analysis
SVM	Support vector machines
RaF	Standard Random Forest
DRaF	Standard double Random Forest
MPSVM	Multisurface proximal support vector machines
RaF-PCA	Principal component analysis based ensemble of decision trees
RaF-LDA	Linear discriminant analysis based ensemble of decision trees
MPRaF-T	MPSVM based oblique decision tree ensemble with Tikhonov regularization
MPRaF-P	MPSVM based oblique decision tree ensemble with axis parallel regularization
MPRaF-N	MPSVM based oblique decision tree ensemble with NULL space regularization
DRaF-PCA	Rotation based double random forest with principal component analysis
DRaF-LDA	Rotation based double random forest with linear discriminant analysis
MPDRaF-T	Oblique double random forest with MPSVM via Tikhonov regularization
MPDRaF-P	Oblique double random forest with MPSVM via axis parallel regularization
MPDRaF-N	Oblique double random forest with MPSVM via NULL space regularization

perturbed training sets generated from a given training set and variance measure is how much the base learners guess fluctuates with the perturbations of the given training set.

Decision tree algorithm is a commonly used classification model due to its simplicity and better interpretability. Decision tree uses divide and conquer approach to recursively partition the data. The recursive partition of the tree is sensitive to perturbation of the input data, and results in an unstable classifier. Hence, it is said to have high variance and low bias. The ensemble methodology can be used in unstable classifiers to further improve the classification performance.

Random forest (Breiman, 2001) and rotation forest (Rodriguez, Kuncheva, & Alonso, 2006) are the well-known classification models, widely used in the literature. Both these models are based on the ensemble methodology and use decision tree as the base classifier. Due to the better generalization performance, random forest proved to be one of the best classification models among 179 classifiers evaluated on 121 datasets (Fernández-Delgado, Cernadas, Barro, & Amorim, 2014).

An ensemble of decision trees, Random forest, uses bagging (Breiman, 1996b) and random subspace (Ho, 1998) strategy. These two approaches induce diversity among the base learners, here decision trees, for better generalization. Bagging, also known as bootstrap aggregation, generates multiple bags of a given training set such that each decision tree is trained on a given bag of the data. Each tree uses a bag of training data whose distribution is akin to the whole population and hence, each classifier shows good generalization performance. Within each decision tree, random subspace approach is used in each non-terminal node to further boost the diversity among the base models. Random forest has been successfully applied for analysis of gene expression data (Jiang et al., 2004), EEG classification (Shen, Ong, Li, Hui, & Wilder-Smith, 2007), spectral data classification (Menze et al., 2009), recognition of objects, image segmentation (Ho, 1998; Hothorn, Leisch, Zeileis, & Hornik, 2005) and chimera identification (Ganaie, Ghosh, Mendola, Tanveer & Jalan, 2020). Other applications include selection of features (Menze et al., 2009), analysis of sample proximities (Menze, Petrich, & Hamprecht, 2007) and so on. Random forest have also been adapted to Spark based distributed and scalable environments (Lulli, Oneto, & Anguita, 2017a, 2017b). With the growing of privacy concerns, Random forest models have been improved to meet the privacy expectations. Differential privacy (Dwork, 2008) has been widely adopted in Random Forest (Fletcher & Islam, 2017; Guan, Sun, Shi, Wu, & Du, 2020; Patil & Singh, 2014; Xin, Yang, Wang, & Huang, 2019).

To obtain the better generalization performance, various hyperparameters of the random forest need to be chosen optimally. These hyperparameters include number of base learners (here, decision trees) in a forest (ntree), number of candidate features for evaluation at a given non-leaf node (mtry), and number of samples in an impure node (nodesize or minleaf) (we will use minleaf and nodesize interchangeably). To get these parameters optimally, different studies have been proposed. Analysis of tuning process (Freeman, Moisen, Coulston, & Wilson, 2016; Probst & Boulesteix, 2017), sensitivity of the parameters (Huang & Boutros, 2016), effect of number of trees in an ensemble (Banfield, Hall, Bowyer, & Kegelmeyer, 2006; Hernández-Lobato, MartíNez-MuñOz, & Suárez, 2013; Oshiro, Perez, & Baranauskas, 2012) provide insight how these parameters affect the model performance. To obtain the optimal number of candidate features, different methods (Boulesteix, Janitza, Kruppa, & König, 2012; Han & Kim, 2019) have been proposed. Analysis of optimal sample size in bagging (Martínez-Muñoz & Suárez, 2010) and estimation of tree size via combination of random forest with adaptive nearest neighbors (Lin & Jeon, 2006) result in the better choice of the hyperparameters.

Broadly speaking, there are two approaches, namely, univariate decision trees (Banfield et al., 2006) and multivariate decision trees (Murthy & Salzberg, 1995) for generating the decision trees. Univariate decision trees, also known as axis parallel or orthogonal decision trees, use some impurity criteria to optimize best univariate split feature among the set of randomly chosen subspace of features. Multivariate decision trees, also known as oblique decision trees, perform the node splitting using all or a part of the features. In general, decision boundary of an oblique decision tree can be approximated by a large number of stair-like decision boundaries of the univariate decision trees.

Random forest is a univariate model and builds hyperplane at each non-terminal node such that splitting at the children nodes is easier in a given decision tree. At a given non-leaf node, the splitting hyperplane may not be a good classifier (Manwani & Sastry, 2011). Different criteria like entropy measure, Gini index measure and twoing rule are involved in most of the decision tree based models for choosing the best split among the set of splits such that the best split results in lowest impurity score. At each non-leaf node, impurity criteria measures skewness of the distribution of the different category samples. Nearly uniform distribution is assigned low impurity score while as high impurity score is given to a distribution wherein the samples of a particular class dominate the other classes. In most of the decision tree based induction tree algorithms, some impurity measure is optimized for generating the tree. However, due to non differentiability of the impurity measures with respect to the hyperplane parameters, different search techniques are employed for generating the decision trees. Like deterministic hill-climbing model in CART-LC (Breiman, Friedman, Stone, & Olshen, 1984), randomized search based CART-LC in OC1 (Murthy, Kasif, Salzberg, & Beigel,

1993). In high dimensional feature space, both these methods suffer due to searching in 1-D at a time and local optimum problem. Thus, to avoid the local optima, multiple trails or restarts are used to minimize the chances of ending up with the local optima. Evolutionary approaches have also been used for optimizing in all dimensions (Cha & Tappert, 2009; Pedrycz & Sosnowski, 2005) which tolerate the noisy evaluation of a rating function and also simultaneously optimize the multiple rating functions (Cantu-Paz & Kamath, 2003; Pangilinan & Janssens, 2011). Extremely randomized trees (Geurts et al., 2006) and its oblique version (Zhang, Ren, & Suganthan, 2014), strongly randomized the attribute set and its cut point. Other approaches include fuzzy based decision trees (Wang & Dong, 2008; Wang, Zhai, & Lu, 2008), ensemble of feature spaces (Zhang & Suganthan, 2014b) and decision tree support vector machine (Zhang, Zhou, Su, & Jiao, 2007). Random feature weights for decision tree ensemble (Maudes, Rodríguez, García-Osorio, & García-Pedrajas, 2012) associates weight to each attribute for better diversity of the model. Recent studies have evaluated the interpretability of the decision forests so that the decisions can be interpreted for better understanding (Fernández, de Diego, Aceña, Fernández-Isabel, & Moguerza, 2020; Sagi & Rokach, 2020). For more literature about the decision trees, we refer the readers to Rokach (2016).

With all the impurity measures, given in Manwani and Sastry (2011), the issue is they are function of different class distributions on each side of the hyperplane and ignore the geometric structure of the class regions (Manwani & Sastry, 2011) as if the impurity measure is unaffected if one changes the data labels without any change in the relevant features of each category on either side of the hyperplane.

To incorporate the geometric structure of class distributions, support vector machines (SVM) (Cortes & Vapnik, 1995) are employed to generate the decision trees (Manwani & Sastry, 2011). The multisurface proximal support vector machines (MPSVM) (Mangasarian & Wild, 2005) generate the proximal hyperplanes in a manner that each plane is proximal to the samples of one class and farthest from the samples of another class. Manwani and Sastry (2011) generated the two clustering planes at each non-leaf node and choose the angle bisector of these planes which makes the nodes pure. MPSVM is a binary class algorithm, hence, they decomposed the multiclass problem into a binary class by grouping the majority class samples into one class and rest samples into other class. As the node becomes purer with the growth of a tree, the subsequent nodes receive smaller number of samples. To avoid this problem, NULL space method (Chen, Liao, Ko, Lin, & Yu, 2000) is used in Manwani and Sastry (2011). Also, MPSVM based oblique decision tree ensemble (Zhang & Suganthan, 2014a) employed regularization approaches like Tikhonov regularization (Marroquin, Mitter, & Poggio, 1987) and axis-parallel split regularization. In Ganaie, Tanveer and Suganthan (2020), twin bounded SVM (Shao, Zhang, Wang, & Deng, 2011) resulted in more generalization performance as no explicit regularization methods are needed to handle these problems. Both MPSVM based oblique decision tree ensemble (Zhang & Suganthan, 2014a) and TBSVM based oblique decision tree ensemble (Zhang & Suganthan, 2014a) use single base learner at each nonleaf node to search the optimal split among the candidate splits. The oblique decision tree ensemble showed better generalization than the standard random forest (Zhang & Suganthan, 2017). Heterogeneous oblique random forest (Katuwal, Suganthan, & Zhang, 2020) generates hyperplanes via MPSVM, logistic regression, linear discriminant analysis, least squares SVM and ridge regression. The optimal hyperplane for best split is chosen among the generated planes which results in purer nodes.

Recent study of double random forest (Han, Kim, & Lee, 2020) evaluated the effect of node size on the performance of the model. The study revealed that the prediction performance may improve if deeper decision trees are generated. The authors showed that the largest tree grown on a given data by the standard random forest might not be sufficiently large to give the optimal performance. Hence, double random forest (Han et al., 2020) generated decision trees that are bigger than the ones in standard random forest. The maximum performance of the random forest is achieved corresponding to the minimum node size which generates the larger trees (Zhang & Suganthan, 2014a). This supports the hypothesis that larger the trees of an ensemble the better the performance of the model is. Instead of training each decision tree with different bags of training set obtained via bagging approach at the root node, Han et al. (2020) generated each tree with the original training set and used bootstrap aggregation at each non-terminal node of the decision tree to obtain the best split. However, both the random forest and double random forest are univariate decision trees and hence ignore the geometric class distributions resulting in lower generalization performance. To overcome these issues, we propose oblique double random forest. Oblique double random forest models integrate the benefits of double random forest and the geometric structure information of the class distribution for better generalization performance. For generating more diverse ensemble learners in the double random forest, feature space is rotated or transformed at each non leaf node using two transformations known as linear discriminant analysis and principal component analysis. Using transformations at each non-leaf node on different randomly chosen feature subspaces improves diversity among the base models and leads to better generalization performance.

The main highlights of this paper are:

- We use different rotations (principal component analysis and linear discriminant analysis) at each non-leaf node to generate diverse double random forest ensembles (DRaF-PCA and DRaF-LDA).
- The proposed oblique double random forest (MPDRaF-T, MPDRaF-P and MPDRaF-N) variants use MPSVM for obtaining the optimal separating hyperplanes at each non-terminal node of the decision tree ensembles.
- The proposed ensemble of double Random forest generate larger trees compared to the variants of standard Random forest.
- Statistical analysis reveals that the average rank of the proposed double random forest models is superior than the standard random forest. Moreover, the average accuracy of the proposed DRaF-LDA, DRaF-PCA, and MPDRaF-P is superior than the standard random forest and standard double random forest models. Also, the average rank of the proposed DRaF-LDA, MPDRaF-P and DRaF-PCA is better compared to the standard double Random forest.

2. Related work

In this section, we briefly review the related work of the ensemble of decision trees.

2.1. Handling multiclass problems

MPSVM is a binary classification model and finding the optimal separating hyperplanes at each non-terminal node of a decision tree may be a multiclass problem. To handle the multiclass problem via binary class approach, different methods like one-versus-all (Bottou et al., 1994), one-versus-one (Knerr, Personnaz, & Dreyfus, 1990), decision directed acyclic graph (Platt, Cristianini, & Shawe-Taylor, 1999), error correcting output codes (Dietterich & Bakiri, 1994) and so on have been proposed. Data partitioning rule of the decision trees at each non-leaf node

proves handy over other binary classification models (Zhang & Suganthan, 2014a). Separating the classes with majority samples as one class and rest samples as another class results in an inefficient model as it fails to capture the geometric structure of the data samples (Manwani & Sastry, 2011). To incorporate the geometric structure, the authors in Zhang and Suganthan (2014a) decomposed the multiclass problem into a binary one by using class separability information. The authors used Bhattacharyya distance for decomposition. In statistics, Bhattacharyya distance gives the measure of similarity between the two discrete probability distributions or continuous probability distributions as it is deemed to be a good insight about separability of classes between two normal classes $C_1 \sim N(\mu_1, \nu_1)$, $C_2 \sim N(\mu_2, \nu_2)$, where μ_i and ν_i are the parameters of the normal distribution of class C_i, for $i = 1, 2$. Following the similar approach as in Zhang and Suganthan (2014a), we used multivariate Gaussian distribution (Jiang, 2011). Motivated by Jiang (2011) and Zhang and Suganthan (2014a), we use Bhattacharyya distance to measure the class separability for decomposing the multiclass problem into a binary class problem (Algorithm 1).

Algorithm 1 Decomposition of Multiclass problem to a binary class problem

Input:

$D := N \times n$ be the training dataset with N number of data points with feature size n.

$Y := N \times 1$ be the target labels.

$\{L_1, L_2, \ldots, L_C\}$ be the target labels.

Output:

C_p and C_n are two hyperclasses or groups

For each class $j = 1, 2, \ldots, C$.

1. For each pair of L_j and L_k, for $k = j+1, \ldots, C$ as:

$$F(L_j, L_k) = \frac{1}{8}(\mu_k - \mu_j)^t \left(\frac{\nu_j + \nu_k}{2}\right)^{-1} (\mu_k - \mu_j) + \frac{1}{2} ln \frac{|(\nu_j + \nu_k)/2|}{\sqrt{|\nu_j||\nu_k|}} \tag{1}$$

2. Find the pair L_p and L_n of classes with the maximum Bhattacharyya distance, and assign them to C_p and C_n respectively.
3. For every other class, if $F(L_k, L_p) < F(L_k, L_n)$ then group L_k to C_p otherwise group in C_n.

2.2. Multisurface proximal support vector machine

Multisurface proximal support vector machine (MPSVM) (Mangasarian & Wild, 2005) is a binary class algorithm. Suppose X_1, X_2 be the data points belonging to the positive and negative class, respectively. Here, $X_1 \in \mathbb{R}^{m_1 \times n}$, $X_2 \in \mathbb{R}^{m_2 \times n}$ and each sample $x \in \mathbb{R}^n$. MPSVM generates two hyperplanes as

$$x^t w_1 - b_1 = 0 \quad \text{and} \quad x^t w_2 - b_2 = 0, \tag{2}$$

where (w_1, b_1) and (w_2, b_2) are the planes closer to the samples of positive and negative class, respectively. MPSVM minimizes the sum of squared two norm distances between the samples of positive class divided by the sum of squared distances from the samples of negative class to the plane. Thus, the optimization problems of MPSVM are given as follows:

$$\min_{(w,b)\neq 0} \frac{\|X_1 w - eb\|^2 / \left\|\begin{matrix} w \\ b \end{matrix}\right\|^2}{\|X_2 w - eb\|^2 / \left\|\begin{matrix} w \\ b \end{matrix}\right\|^2} \tag{3}$$

and

$$\min_{(w,b)\neq 0} \frac{\|X_2 w - eb\|^2 / \left\|\begin{matrix} w \\ b \end{matrix}\right\|^2}{\|X_1 w - eb\|^2 / \left\|\begin{matrix} w \\ b \end{matrix}\right\|^2}, \tag{4}$$

where $\|\cdot\|$ is a two norm, e is a vector of ones with appropriate dimensions.

Suppose

$$P = \begin{bmatrix} X_1 & -e \end{bmatrix}^t \begin{bmatrix} X_1 & -e \end{bmatrix}, Q = \begin{bmatrix} X_2 & -e \end{bmatrix}^t \begin{bmatrix} X_2 & -e \end{bmatrix}, r = \begin{bmatrix} w \\ b \end{bmatrix}, \tag{5}$$

then the optimization problem (3) is given as

$$\min_{r\neq 0} \frac{r^t P r}{r^t Q r}. \tag{6}$$

Similarly, the optimization problem (4) is given as follows:

$$\min_{r\neq 0} \frac{r^t S r}{r^t U r}, \tag{7}$$

where $S = \begin{bmatrix} X_2 & -e \end{bmatrix}^t \begin{bmatrix} X_2 & -e \end{bmatrix}$ and $U = \begin{bmatrix} X_1 & -e \end{bmatrix}^t \begin{bmatrix} X_1 & -e \end{bmatrix}$.

The clustering hyperplanes are obtained by solving the following generalized eigenvalue problems:

$$Pr = \lambda Q r, \ r \neq 0 \tag{8}$$

$$Sr = \gamma U r, \ r \neq 0. \tag{9}$$

The optimal hyperplanes are the eigenvectors corresponding to the smallest eigenvalues.

The way (8) and (9) are defined, the clustering hyperplanes are able to capture the geometric properties of the data which are helpful while discriminating among the classes.

2.2.1. Random forest

Random forest (Breiman, 2001) is an ensemble with decision tree as the base learner which are generated using the concept of bagging and random subspace method. Both bagging and random subspace methods induce diversity among the decision trees of an ensemble. Each decision tree of an ensemble chooses the optimal split among the randomly selected candidate feature subsets at a given non-leaf node. The optimal split is chosen using some impurity criterion's like information gain, Gini impurity and so on Breiman et al. (1984).

The algorithm of the random forest is given in Algorithm 2. The classification and regression tree (CART) (Breiman, 2001) performs the test split using only one feature and hence, known as univariate decision tree (Murthy & Salzberg, 1995).

2.3. Double random forest

Double random forest (Han et al., 2020) is an ensemble with decision tree as the base learner which uses the concept of bagging and the random subspace method. Unlike standard random forest wherein the base learner is trained on the boostrapped sample of the dataset, double random forest trains each base learner on the original dataset. This results in more unique features in the data used in training the double random forest than standard forest. The more number of unique instances leads to larger decision trees and hence better generalization performance. Double random forest uses bootstrap sampling momentarily at every non-terminal node. Once the feature which gives the split is chosen among the randomly chosen subset of the features from the bootstrap samples, the splitting of the original data is done and hence original data is sent down the decision

Algorithm 2 Random Forest

Training Phase:
Given:

$D := N \times n$ be the training dataset with N number of data points with feature size n.
$Y := N \times 1$ be the target labels.
L : is number of base learners.
"mtry": number of candidate features to be evaluated at each non-leaf node.
"nodesize" or *"minleaf"*: maximum number of samples in an impure node.

For each decision tree, T_i for $i = 1, 2, \ldots, L$

1. Generate bootstrap samples D_i from D.
2. Generate the decision tree using D_i:
   For a given node d:
   (i) Choose *"mtry"*$= \sqrt{n}$ number of features from the given feature space of D_i.
   (ii) Select the best feature split feature and the cutpoint among the random feature subset.
   (iii) With the optimal split feature and the cutpoint, divide the data.

   Repeat steps (i)–(iii), until the stopping criteria is met.

Classification Phase:
For a test data point x_i, use the base learner of the forest to generate the label of the test sample. The predicted label of the test data point is given by the majority voting of the decision trees of an ensemble.

tree resulting in more number of unique instances. The algorithm of the double random forest is given in Algorithm 3.

3. Proposed oblique and rotation double random forest

This paper proposes two approaches for generating the oblique and rotation double random forest known as oblique double random forest models and the rotation based double random forest models. Two approaches are given as follows:

3.1. Oblique double random forest with MPSVM

Univariate decision trees do not capture properties of the data geometrically. Both standard random forest and double random forest are univariate decision tree ensembles. Also, decision trees in the standard random forest may not be large enough for the datasets to get the better generalization. To overcome these limitations, we propose oblique double random forest with MPSVM. Unlike standard random forest, the oblique double random forest models with MPSVM use bootstrapping samples at every non-terminal node (until some condition is met as given in Algorithm 5) for generating the optimal oblique splits and divide the original data instead of bootstrapped samples among the children nodes. To incorporate the geometric structure in the splitting hyperplane, the proposed oblique double random forest uses MPSVM wherein optimal split at each non-leaf node is generated based on the clustering hyperplanes. As the decision tree size increases, the data points arriving at a particular node decreases and hence, the issues of sample size may arise. To overcome this issue, we use different regularization techniques to obtain a better generalization performance. The regularization approaches used are Tikhonov regularization, axis parallel split regularization

Algorithm 3 Double Random Forest

Training Phase:
Given:
$D := N \times n$ be the training dataset with N number of data points with feature size n.
$D_i := N_i \times n_i$ be the training samples reaching to a node i, with N_i number of samples with feature size n.
$Y := N \times 1$ be the target labels.
L : is number of base learners.
"mtry": number of candidate features to be evaluated at each non-leaf node.
"nodesize" or *"minleaf"*: maximum number of data samples to be placed in an impure node.

For each decision tree, T_i for $i = 1, 2, \ldots, L$

1. Use training data D.
2. Generate the decision tree T_i with randomly chosen subset of features and randomized bootstrap instance using D:
   For a given node d with data D_d:
   (i) if $N_d > N \times 0.1$
   Generate bootstrap sample D_d^* from D_d.
   else
   $D_d^* = D_d$
   (i) Choose *"mtry"*$= \sqrt{n}$ number of features from the given feature space of D_d^*.
   (ii) Select the best split feature and the cutpoint among the random feature subset D_d^*.
   (iii) With the optimal split feature and the cutpoint with D_d^*, split the data D_d into child nodes.

   Repeat steps (i)–(iii), until either of the satisfied:

   - Node reaches to purest form.
   - Samples reaching a given node are lesser or equal than *minleaf*

Classification Phase:
For a test data point x_i, use the decision trees of the forest to generate the label of the test sample. The predicted class of the test data point is given by the majority voting of the decision trees of an ensemble.

Algorithm 4 Null Space Regularization

Input: P (Positive class) and H (Negative class) as given in (5).
Output: Clustering hyperplane $\begin{bmatrix} w \\ b \end{bmatrix}$.

1. Suppose P is rank deficit with rank $r < n+1$, calculate $O = [\alpha_1, \alpha_2, \cdots, \alpha_{n+1-r}]$ whose columns are the orthonormal basis for the Null space of P.
2. Project the matrix Q in the Null space of P. For each vector (row) p in matrix P, the projection is given as pOO^t. Hence, the projection of matrix Q is given as $\bar{Q} = \sum_{p \in Q} OO^t p^t pOO^t = OO^t QOO^t$. In the similar manner, the projection of matrix P is given as $\bar{P} = OO^t POO^t$.
3. Since the columns of O span the Null space of P, hence $\bar{P}$ would be zero. Thus, the desired plane is the eigen vector corresponding to the largest eigenvector of $\bar{Q}$.

and null space approach. If the model uses Tikhonov regularization then the proposed model is named as oblique double random forest via MPSVM with Tikhonov regularization (MPDRaF-T), if

the model uses axis parallel split regularization then the proposed model is known as oblique double random forest via MPSVM with axis parallel split regularization (MPDRaF-P) and if the model uses null space approach then the proposed model is known as oblique double random forest via MPSVM with null space approach (MPDRaF-N). In Tikhonov regularization, the small positive number is added along the diagonal elements to regularize the data matrix (say, H) i.e., if data matrix H is rank deficient, then regularize H as:

$$H = H + \delta \times I, \tag{10}$$

where δ is a small positive number and I is appropriate dimensional identity matrix. In axis-parallel split regularization, if the data matrix (say, H) is rank deficient at a given node then we follow axis parallel approach to complete the growth of decision tree. Thus, heterogeneous test functions are used for growing the decision trees. i.e., till the current node MPSVM is used for generating the optimal splits and now onwards axis parallel approach is followed for growing the decision tree. In order to handle the sampling issues, Manwani and Sastry (2011) proposed the Null space approach (given in Algorithm 4) for regularizing the matrices. For the proposed MPDRaF-N, we follow the Algorithm 4 for regularizing the matrices.

Algorithm 5 summarizes the oblique double random forest with MPSVM.

3.2. Double random forest with PCA/LDA

For generating the diverse learners in an ensemble, we propose rotation based double random forest ensemble models. Rotation or transformation on different random feature subspaces results in different projections leading to better generalization performance. In this method, the objective is to rotate or transform the data for better diversity among the base learners. At each non-leaf node, the rotation is applied on random feature subspace which results in improved diversity among the base classifiers. We use two approaches for rotation of feature subspace i.e., principal component analysis (PCA) and linear discriminant analysis (LDA).

The proposed double random forest with PCA (DRaF-PCA) is given in Algorithm 6. At each non-leaf node, rotation or transformation is applied on the bootstrapped samples reaching a given node with random feature subspace.

The algorithm of the proposed double random forest with LDA (DRaF-LDA) varies from Algorithm 6 at step (*ii*) and (*iii*). In DRaF-LDA model, instead of calculating total scatter matrix S_d at each node, within class scatter matrix S_d^w and between class scatter matrix S_d^b are calculated. Then, generalized eigenvectors of (S_d^w, S_d^b) are calculated ($S_d^b \times \alpha = \lambda \times S_d^w$, where α is the generalized eigenvector corresponding to the generalized eigenvalue λ).

Algorithm 5 Oblique Double Random Forest with MPSVM

Training Phase:

Given:

$D := N \times n$ be the training set with N number of samples with feature size n.

$D_i := N_i \times n_i$ be the training samples reaching to a node i, with N_i number of samples with feature size n_i.

$Y := N \times 1$ be the target labels.

L : is number of base learners.

"mtry": number of candidate features to be evaluated at each non-leaf node.

"nodesize" or *"minleaf"*: maximum number of data samples to be placed in an impure node.

For each decision tree, T_i for $i = 1, 2, \ldots, L$

1. Use training data D.
2. Generate the decision tree T_i with randomly chosen subset of features and randomized bootstrap instance using D:
   For a given node d with data D_d:
   (i) if $N_d > N \times 0.1$
   Generate bootstrap sample D_d^* from D_d.
   else
   $D_d^* = D_d$
   (i) Choose *"mtry"*$= \sqrt{n}$ number of features from the given feature space of D_d^*
   (ii) Using Algorithm 1 group the dataset D_d^* into C_p and C_n.
   (iii) Use MPSVM (with different regularization's) for generating the optimal split with C_p and C_n as input, and split the data D_d into child nodes.

   Repeat steps (i)–(iii), until the stopping criteria is one of the conditions is met:

   - Node reaches to purest form.
   - Samples reaching a given node are lesser or equal than *minleaf*

Classification Phase:

For a test data point x_i, use the decision trees of the forest to generate the label of the test sample. The predicted class of the test data point is given by the majority voting of the decision trees of an ensemble.

4. Comparison of the proposed oblique and rotation based double random forest models with the existing baseline models

The main differences of the proposed models with respect to the existing models are given as follows:

1. MPDRaF-T, P, *N* are the oblique double random forest variants which employ bagging at each non leaf node to allow the generation of bigger trees. Unlike standard variants like RaF, MPRaF-T, MPRaF-P and MPRaF-N, the proposed models use the training bags which have more unique instances of the samples which results in generation of bigger trees. Moreover, MPDRaF-T,P,N capture the geometric properties of the data which is ignored by the standard RaF and double RaF models.
2. The standard RaF and DRaF models use the concepts of random subspace and bagging for introducing the diversity among the base learners of an ensemble. However, the proposed DRaF-PCA and DRaF-LDA employ PCA and LDA transformations at non-leaf nodes in addition to the random subspace and bagging concepts for producing more diverse base learners. Thus, the proposed DRaF-PCA and DRaF-LDA models possess better diversity compared to the RaF and DRaF models. Unlike RaF-PCA and RaF-LDA, the proposed DRaF-PCA and DRaF-LDA models use bagging concept at each non-leaf node which allow greater depth of the tree and hence better performance.

5. Experimental analysis

Here, we discuss the setup followed in experiments and analyze the performance of the proposed oblique and rotation double random models and baseline models or existing models (here, standard RaF, Breiman, 2001, standard DRaF, Han et al., 2020, MPRaF-T, Zhang & Suganthan, 2014a, MPRaF-P, Zhang &

Algorithm 6 Double Random Forest with PCA

Training Phase:
Given:
$D := N \times n$ be the training set with N number of samples with feature size n.
$D_i := N_i \times n_i$ be the training samples reaching to a node i, with N_i number of samples with feature size n_i.
$Y := N \times 1$ be the target labels.
L : is number of base learners.
"*mtry*": number of candidate features to be evaluated at each non-leaf node.
"*nodesize*" or "*minleaf*": maximum number of data samples to be placed in an impure node.

For each decision tree, T_i for $i = 1, 2, \ldots, L$

1. Use training data D.
2. Generate the decision tree T_i with randomly chosen subset of features and randomized bootstrap instance using D:
   For a given node d with data D_d:
   (i) if $N_d > N \times 0.1$
   Generate bootstrap sample D_d^* from D_d.
   else
   $D_d^* = D_d$
   (i) Choose "*mtry*"$= \sqrt{n}$ number of features from the given feature space of D_d^*
   (ii) Calculate total scatter matrix S_d using D_d^*.
   (iii) Calculate all the eigenvectors of S_d, denoted by V.
   (iv) Calculate the data transformation using all the eigenvectors V as, $D_{PCA}^* = D_d^* * V$.
   (v) In the PCA space, search the best feature split.
   (iii) With the optimal split feature and the cutpoint, split the data D_d into the child nodes.

   Repeat steps (i)–(iii), until the stopping criteria is met.

Classification Phase:
For a test sample x_i, generate labels via decision trees of the forest. At every non-terminal node, the test data sample is rotated with the same matrix V generated in the training stage. The predicted class of the test data point is given by the majority voting of decision trees of an ensemble.

Suganthan, 2014a, MPRaF-N, Zhang & Suganthan, 2014a, RaF-PCA, Zhang & Suganthan, 2014b and RaF-LDA, Zhang & Suganthan, 2014b).

5.1. Experimental setup

We evaluated the classification models on UCI datasets (Dua & Graff, 2017) and real world fisheries datasets (González-Rufino, Carrión, Cernadas, Fernández-Delgado, & Domínguez-Petit, 2013). We follow the preprocessing scripts of Klambauer, Unterthiner, Mayr, and Hochreiter (2017) wherein the partitions of the training and testing sets are publicly available for evaluation. Table 1 of the supplementary file summarizes the details of the 121 datasets used for evaluation. The sample size of the datasets varies from 10 to 130064. Also, the dimensions of the feature samples vary from 3 to 262 and the number of classes vary from 2 to 100.

In all the ensemble models, 50 is the number of base learners. At each non-terminal node, we evaluated $\sqrt{n}$ number of features, here n is the dimension of feature set and the minleaf parameter is set to default. We used CART (Breiman et al., 1984) as the base classifier.

5.2. Statistical analysis

Table 2 summarizes the classification performance of each ensemble model on 121 datasets. From the given table, it is evident that the average accuracy of the proposed DRaF-LDA, MPDRaF-P and DRaF-PCA are superior compared to the existing classifiers. Following Fernández-Delgado et al. (2014), we rank each classifier based on its performance on each dataset. Every classifier in Friedman test is given a rank on a dataset with the worse performing classifier assigned higher rank and vice versa. Hence, a lower rank indicates better generalization performance of the model. The average rank of each classification model is presented in Table 3. It is evident that the average rank of the proposed ensemble models DRaF-LDA, DRaF-PCA, and MPDRaF-P is better as compared to all the existing classifiers. Furthermore, the rank of the proposed MPDRaF-T is better in comparison to existing classifiers (except standard DRaF and DRaF-LDA).

For evaluation of the models via statistical tests, we perform statistical analysis. We used Friedman test (Demšar, 2006) with corresponding Nemenyi post hoc test for the comparison of the models. Let r_i^j be the rank of the jth classification model assigned on the ith dataset among the N datasets. In the Friedman test, average rank $\sum_i r_i^j$ is used for the evaluation of the classification models. When the number of datasets (N) and the number of classifiers (n) are large enough, then the Friedman statistic given as:

$$\chi_F^2 = \frac{12N}{n(n+1)}\left[\sum_j R_j^2 - \frac{n(n+1)^2}{4}\right] \tag{11}$$

follows χ_F^2 distribution with $(n-1)$ degrees of freedom under null hypothesis. As χ_F^2 is undesirably conservative, hence, a better statistic is given as:

$$F_F = \frac{(N-1)\chi_F^2}{N(n-1)-\chi_F^2} \tag{12}$$

follows $F-$distribution with $(n-1)$ and $(n-1)(N-1)$ degrees of freedom. Under the null hypothesis, all the classifiers are equal, hence, the ranks of the classifiers are equal. If the null-hypothesis fails, Nemenyi post-hoc test (Nemenyi, 1962) gives pairwise performance evaluation of the classifiers. Two classifiers are significantly different if their average ranks differ by at least the critical difference:

$$CD = q_\alpha \sqrt{\frac{n(n+1)}{6N}} \tag{13}$$

where α is the level of significance and q_α is the studentized range statistic divided by $\sqrt{2}$.

The average ranks of the classification models RaF, MPRaF-T, MPRaF-P, MPRaF-N, RaF-PCA, RaF-LDA, DRaF, MPDRaF-T, MPDRaF-P, MPDRaF-N, DRaF-PCA and DRaF-LDA are 6.99, 6.81, 6.48, 8, 7.31, 6.12, 6.27, 6.38, 5.45, 7.3, 5.84 and 5.04 respectively. With simple calculations, we get $\chi_F^2 = 71.0559$ and $F_F = 6.7675$. At 5% level of significance i.e. $\alpha = 5\%$, F_F follows F-distribution with $(n-1) = 11$ and $(n-1)(N-1) = 1320$. From Statistical table, $F_F(11, 1320) = 1.8$. Since $6.7675 > 1.8$, hence we reject the null hypothesis. Thus, significant difference exists among the classification models. To get the significant difference, we use Nemenyi post hoc test. With simple calculations, critical difference $CD = 1.5149$ with $q_\alpha = 3.268$ at 5% level of significance. From Fig. 1, one can see the statistically significant difference exists among the models which are not connected by a line. Table 1 summarizes the Nemenyi post-hoc test results. From the table, it is evident that the proposed DRaF-LDA is significantly better in comparison to RaF, MPRaF-T, MPRaF-N, RaF-PCA and MPDRaF-N classifiers. Also, the proposed DRaF-PCA is significantly better compared to the DRaF-PCA model.

Table 1
Significance difference of classification performance of the baseline models and the proposed oblique and rotation double random forest with Nemenyi posthoc tests based on the accuracy.

	RaF	MPRaF-T	MPRaF-P	MPRaF-N	RaF-PCA	RaF-LDA	DRaF	MPDRaF-T	MPDRaF-P	MPDRaF-N	DRaF-PCA	DRaF-LDA
RaF									$r-$			$r-$
MPRaF-T												$r-$
MPRaF-P				$r+$								
MPRaF-N			$r-$			$r-$	$r-$	$r-$	$r-$		$r-$	$r-$
RaF-PCA									$r-$			$r-$
RaF-LDA				$r+$								
DRaF				$r+$								
MPDRaF-T				$r+$								
MPDRaF-P	$r+$			$r+$	$r+$					$r+$		
MPDRaF-N									$r-$			$r-$
DRaF-PCA				$r+$								
DRaF-LDA	$r+$	$r+$		$r+$	$r+$					$r+$		

Here, $r+$ denotes that the row model is significantly better than the column model. $r-$ denotes that the row model is significantly worse than the corresponding column model. Empty entries denote that no significant difference exists among the models of a cell.

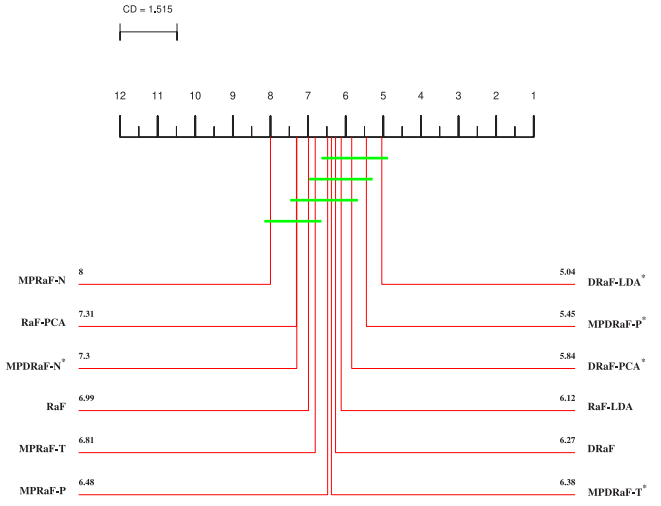

Fig. 1. Nemenyi test based post hoc evaluation of classification models at $\alpha = 5\%$ level of significance. The classification models which are not statistically different are connected.

The decision boundaries corresponding to the spiral dataset generated by the different classifiers are shown in Figure 5 of the supplementary file.

5.3. Win–tie–loss: Sign test

Under the null hypothesis, the pair of classifiers is significantly different if each classification model wins $N/2$ in N datasets. The number of wins follow binomial distribution. When N is large enough, the number of wins follow $N(N/2, \sqrt{N}/2)$, and hence, z-test can be used: two models are significantly better with $p <$ 0.05 if any model has least $N/2 + 1.96\sqrt{N}/2$ wins. Since tied matches favor of null hypothesis, hence, we split the number of ties between the models evenly and if the number is odd we ignore one.

Table 4 summarizes the count of win–tie–loss results among the given classification models. One can see that the proposed rotation double random forest (DRaF-PCA and DRaF-LDA) achieved more wins as compared to the existing models. Compared to the existing MPRaF-N and RaF-PCA models, the proposed MPDRaF-N emerged as winner in more datasets. Also, the proposed MPDRaF-P model emerged as the winner in more datasets in comparison to the given baseline models. Table 5 shows that the proposed DRaF-LDA model is significantly better as compared to the RaF, MPRaF-T, MPRaF-N, RaF-PCA, RaF-LDA and DRaF models. The proposed DRaF-PCA model is significantly better compared to the existing MPRaF-N and RaF-PCA models. Also, the proposed MPDRaF-P is significantly better as compared to the existing models except DRaF model.

5.4. Effect of "mtry" parameter

The parameter *"mtry"* denotes the number of candidate features to be evaluated at each non-leaf node. In a given problem, the smaller *"mtry"* results in stronger randomization among the trees and weaker dependency of their structures on the output. However, if the *"mtry"* is small, the random subset of features selected at a given node may fail to get the geometry of the data points. To see the effect of *"mtry"* parameter, we varied it to different values on the datasets given in Fig. 2. From Fig. 2, it is clear that at very low values of *"mtry"*, the performance is lower. However, as the size of the *"mtry"* parameter increases, the performance starts increasing and becomes stable very quickly. Setting *"mtry"* to $round(\sqrt{n})$ leads to satisfactory performance.

5.5. Effect of "minleaf" parameter

In the ensembles of decision tree *"minleaf"* denotes the maximum number of data samples to be placed in an impure node. In general, smaller trees are generated with higher minleaf which results in higher bias and lower variance. Zhang and Zhang (2008) suggested that performance ensembles of decision tree are robust to this parameter while as Lin and Jeon (2006) suggested that its optimal value varies in different situations. To analyze the effect of this parameter, we evaluated the effect of *"minleaf"* parameter with its value varying from 1 to 3 on 120 datasets (leaving miniboone dataset as it took huge time to compute for all these parameters). The average rank of each model across different parameters corresponding to each model are given in Table 6. With $N = 120$, $K = 3$ (as minleaf = 1,2,3), $F_F(2, 238) = 3.03$. Significant difference exist among the different performances based on the minleaf value of the model if $F_F > 3.03$ (Table 6). From the given table, it is clear that significant difference exists among the performances of the all the models (except DRaF-LDA) with different minleaf parameters. However, in most of the cases smaller minleaf parameter results in better performance. This study is in consensus with the observation that decision trees of an ensemble should grow as much as possible for better performance.

5.6. Average number of nodes

As seen in the above section that smaller minleaf results in better performance, hence, the performance of the models can be increased if there is a way to generate the bigger trees (Han et al.,

Table 2
Classification accuracy of RaF (Breiman, 2001), MPRaF-T (Zhang & Suganthan, 2014a), MPRaF-P (Zhang & Suganthan, 2014a), MPRaF-N (Zhang & Suganthan, 2014a), RaF-PCA (Zhang & Suganthan, 2014b), RaF-LDA (Zhang & Suganthan, 2014b), DRaF (Han et al., 2020), MPDRaF-T, MPDRaF-P, MPDRaF-N, DRaF-PCA AND DRaF-LDA classification models.

Datasets	RaF	MPRaF-T	MPRaF-P	MPRaF-N	RaF-PCA	RaF-LDA	DRaF	MPDRaF-T[a]	MPDRaF-P[a]	MPDRaF-N[a]	DRaF-PCA[a]	DRaF-LDA[a]
abalone	64.68	64.99	65.54	65.06	64.85	65.4	64.18	65.33	63.94	65.33	64.06	65.35
acute-inflammation	100	100	100	100	100	100	100	100	100	100	100	100
acute-nephritis	100	100	100	100	100	100	100	100	100	100	100	100
adult	85.79	85.04	85.54	84.5	85.6	85.47	85.63	85.12	85.45	84.41	85.58	85.47
annealing	54.25	76	38.75	76	62.25	65	37	76	56	76	65.25	64
arrhythmia	73.01	63.05	73.23	61.5	65.49	67.04	73.67	63.05	73.89	60.62	70.35	70.35
audiology-std	75	70	76	24	55	48	78	59	78	25	60	58
balance-scale	86.7	89.42	88.94	89.42	88.62	89.42	82.69	87.82	86.86	89.58	85.42	86.38
balloons	81.25	87.5	87.5	93.75	81.25	75	87.5	93.75	81.25	81.25	81.25	87.5
bank	89.6	88.61	89.2	88.63	89.45	89.91	89.93	88.87	89.29	88.83	89.6	89.82
blood	76.6	76.74	77.27	77.81	76.6	77.01	75.67	77.14	75.94	77.14	75.8	76.34
breast-cancer	73.94	73.94	73.94	73.94	76.06	76.76	75.35	73.24	74.65	76.06	72.89	75
breast-cancer-wisc	97.29	97.71	97.43	97	97.14	97.43	97.14	97.86	97.71	97.57	97.43	97.29
breast-cancer-wisc-diag	95.6	96.83	96.83	97.71	95.6	97.01	95.77	97.01	96.65	96.3	96.83	97.01
breast-cancer-wisc-prog	80.1	80.61	79.59	81.12	80.1	80.61	81.63	82.65	82.14	83.67	82.14	82.14
breast-tissue	70.19	69.23	71.15	71.15	73.08	75	73.08	69.23	69.23	68.27	73.08	70.19
car	96.93	95.31	96.99	88.08	96.76	96.76	97.05	95.37	97.8	87.96	97.16	98.15
cardiotocography-10clases	86.11	82.44	85.59	79.8	84.37	84.84	87.15	83.47	86.53	81.87	84.93	85.64
cardiotocography-3clases	94.02	92.75	94.26	91.57	92.33	93.27	94.92	93.22	94.73	92.23	92.7	93.69
chess-krvk	69.6	65.97	70.12	52.02	73.33	71.72	69.92	66.34	71.36	52.22	75.18	73.24
chess-krvkp	98.25	97.97	98.62	97.43	98.25	98.59	98.56	98.53	98.94	97.84	98.75	98.81
congressional-voting	62.39	61.24	61.01	61.24	60.55	61.01	61.7	62.39	61.7	60.78	60.78	61.7
conn-bench-sonar-mines-rocks	76.92	78.37	78.85	78.37	76.44	78.85	79.33	77.4	80.77	79.33	80.77	84.13
conn-bench-vowel-deterding	98.48	99.78	99.13	99.62	99.57	99.46	98.97	100	99.73	99.68	99.95	99.95
connect-4	83.54	76	81.2	75.41	82.63	82.31	84.01	75.91	81.7	75.4	83.37	82.83
contrac	53.94	50.41	53.13	49.8	51.9	50.68	53.33	48.78	51.15	52.31	51.15	51.56
credit-approval	87.5	86.92	86.05	88.08	88.08	87.5	87.5	86.63	87.21	85.61	87.21	87.06
cylinder-bands	81.25	76.17	80.47	73.05	78.71	77.73	82.03	76.95	82.03	79.3	80.86	80.47
dermatology	98.35	98.08	98.35	96.7	97.8	97.8	98.08	97.8	97.8	97.8	97.53	97.25
echocardiogram	84.85	84.85	85.61	84.09	84.09	83.33	84.09	85.61	84.85	84.85	84.09	84.09
ecoli	86.31	87.2	88.99	87.8	87.5	87.5	88.1	86.01	88.1	88.39	86.61	86.61
energy-y1	94.79	92.58	94.92	94.14	94.53	95.7	95.83	92.19	95.96	94.27	96.09	96.22
energy-y2	89.06	89.45	89.84	89.32	89.97	89.71	88.28	89.06	88.8	89.71	89.84	89.45
fertility	88	89	89	88	88	88	88	88	88	88	88	88
flags	67.19	55.21	64.58	56.77	56.25	57.29	66.67	54.69	63.02	54.69	62.5	62.5
glass	73.11	69.34	75.47	70.28	70.75	72.17	76.89	69.34	75.47	67.92	71.7	74.06
haberman-survival	71.05	71.71	71.05	72.37	70.07	71.38	69.74	70.39	69.08	70.72	69.41	68.75
hayes-roth	87.5	86.61	84.82	81.25	89.29	87.5	89.29	85.71	90.18	75	89.29	88.39
heart-cleveland	57.89	61.51	57.57	59.21	58.22	59.21	55.59	59.21	58.22	59.54	60.2	57.57
heart-hungarian	83.9	84.93	84.25	84.25	84.59	84.59	84.25	83.56	83.56	85.27	84.59	84.59
heart-switzerland	41.13	43.55	41.13	44.35	43.55	45.16	41.94	39.52	41.94	41.13	45.97	47.58
heart-va	35.5	34.5	35.5	36.5	34	37.5	36	32.5	36.5	39.5	33.5	34.5
hepatitis	83.33	82.05	82.05	86.54	82.69	84.62	82.69	82.69	81.41	82.69	81.41	80.77
hill-valley	53.84	66.75	63	65.88	64.03	66.25	54.17	70.09	66.79	66.58	67.2	66.75
horse-colic	86.4	86.03	87.87	87.5	82.35	85.29	86.76	83.46	86.76	84.56	80.51	81.62
ilpd-indian-liver	71.4	70.72	71.23	71.23	73.29	71.23	71.23	72.6	72.95	71.23	73.46	71.75
image-segmentation	93.8	94.18	94.75	92.46	94.96	95.07	94.85	94.63	95.15	92.57	95.93	96.06
ionosphere	91.76	93.75	93.47	93.18	94.03	94.6	91.48	93.75	94.03	94.32	94.89	93.18
iris	95.27	97.3	97.3	97.97	95.95	96.62	95.95	97.3	95.95	97.3	96.62	96.62
led-display	74.3	72	73.7	72.4	73.9	73.6	71.7	72.1	72.4	71.2	71.6	72.1
lenses	83.33	79.17	83.33	79.17	79.17	87.5	83.33	79.17	75	83.33	79.17	79.17
letter	95.31	95.35	95.18	94.83	94.74	95.62	95.86	95.85	96	95.02	96.06	96.73
libras	76.94	84.17	79.17	79.44	80.28	81.39	79.72	86.11	84.72	86.67	85.28	85.83
low-res-spect	90.79	91.17	91.35	89.47	90.6	91.54	91.54	91.17	91.73	90.79	91.17	91.35
lung-cancer	46.88	46.88	50	53.13	40.63	43.75	50	31.25	53.13	50	46.88	50
lymphography	79.05	85.14	83.11	83.78	84.46	84.46	85.81	86.49	83.11	85.81	84.46	86.49

(*continued on next page*)

2020). Thus, greater the size of the tree better the performance is. Here, we analyze the size of the tree via number of nodes. Average number of nodes denote that the average number of nodes in an ensemble. Table 7 gives the average of the nodes present in different ensembles of the classification models. From Fig. 3 represents the average of mean nodes in different classification models. Fig. 3, it is clear that double variants of the random forest have higher number of nodes compared to the standard variants of the random forest. Hence, the proposed variants of the double random forest show better performance due to larger size of the trees.

6. Diversity error diagrams

In this section, we analyze the existing baseline models and the proposed oblique and rotation double random forest in terms of "diversity" among the individual decision tree classifiers and their classification accuracy or error. To visualize both the models in terms of these measures, visualization approach known as kappa-error diversity diagrams are used (Margineantu & Dietterich, 1997). Kappa error diagrams use 2*D* plot for visualization of individual accuracy and diversity of the members of the base learner. For L number of base learners (here, decision trees) in

Table 2 (*continued*).

Datasets	RaF	MPRaF-T	MPRaF-P	MPRaF-N	RaF-PCA	RaF-LDA	DRaF	MPDRaF-T[a]	MPDRaF-P[a]	MPDRaF-N[a]	DRaF-PCA[a]	DRaF-LDA[a]
magic	87.01	86.37	86.26	86.69	87.38	87.06	87.19	86.51	86.78	86.88	87.79	87.57
mammographic	81.98	81.67	80.63	81.67	80.63	80.42	79.9	81.46	80.63	81.35	80.1	80.42
miniboone	93.33	93.07	93.24	92.76	93.21	93.46	93.69	93.5	93.64	93.3	93.65	93.88
molec-biol-promoter	84.62	79.81	84.62	82.69	71.15	78.85	91.35	84.62	87.5	80.77	83.65	85.58
molec-biol-splice	94.2	86.57	93.1	85.01	84.1	89.9	94.7	87.23	93.22	87.14	87.05	90.56
monks-1	59.95	60.59	58.39	57.52	58.04	58.16	60.65	60.47	58.8	58.97	58.22	59.32
monks-2	66.78	66.9	66.9	67.01	66.84	67.01	66.55	66.96	66.61	67.13	66.9	66.72
monks-3	53.01	56.6	52.78	54.34	53.36	52.89	52.78	54.17	52.95	52.78	53.01	53.76
mushroom	100	100	100	100	100	100	100	100	100	100	100	100
musk-1	86.13	86.97	83.82	87.18	86.13	83.82	86.34	89.29	86.97	87.82	88.24	85.92
musk-2	97.21	96.12	95.94	95.69	95.98	96.12	98.12	96.53	96.45	96.07	96.71	96.95
nursery	99.28	98.58	99.21	96.74	99.22	99.33	99.31	98.9	99.53	96.95	99.66	99.76
OM_nucleus_4d	77.65	81.57	82.55	80.69	82.55	82.65	79.8	84.31	83.24	82.84	82.45	84.31
OM_states_2f	91.37	91.57	92.16	91.86	91.86	92.16	92.35	92.35	92.35	92.55	92.06	92.45
OT_nucleus_2f	79.39	81.58	82.79	83.11	82.57	82.24	80.7	83.44	82.79	82.89	83.77	83.22
OT_states_5b	90.9	92.54	92	92.65	92.65	93.31	92.21	93.64	93.09	93.09	92.87	93.64
optical	96.08	95.66	96.26	84.65	95.72	91.62	96.91	96.37	96.74	83.85	96.59	94.3
ozone	97.08	97.2	97.16	97.16	97.16	97.16	97.08	97.16	97.16	97.16	97.16	97.2
page-blocks	97.08	96.98	97.3	96.78	97.09	97.13	97.08	97.08	97.09	97.08	97.09	97.28
parkinsons	88.78	92.35	89.8	91.84	87.76	90.82	90.31	92.86	92.35	92.35	90.82	91.84
pendigits	95.05	96.76	95.75	96.06	96.38	96.48	95.48	96.96	96.22	96.18	96.53	96.58
pima	76.69	75.26	75.52	75.13	74.61	74.87	73.96	74.74	74.22	74.48	74.09	75
pittsburg-bridges-MATERIAL	91.35	93.27	91.35	92.31	92.31	92.31	88.46	93.27	89.42	92.31	90.38	91.35
pittsburg-bridges-REL-L	74.04	75.96	73.08	75.96	75	73.08	73.08	74.04	71.15	78.85	73.08	75
pittsburg-bridges-SPAN	61.96	72.83	63.04	67.39	69.57	71.74	60.87	67.39	61.96	67.39	66.3	66.3
pittsburg-bridges-T-OR-D	88	88	88	88	88	90	89	88	88	88	88	88
pittsburg-bridges-TYPE	68.27	69.23	67.31	66.35	71.15	66.35	67.31	69.23	68.27	69.23	70.19	71.15
planning	70	67.78	70	70	70.56	69.44	69.44	71.67	71.11	72.22	70.56	70.56
plant-margin	79.25	75.06	72.25	72.56	76	75.5	81.56	76.88	77.5	73.06	79.75	82.44
plant-shape	59.44	66.13	62.13	65.25	65.31	68.44	61.94	67.75	66.31	66.13	70	73.44
plant-texture	77.94	77.25	76.06	75.06	75.81	76.81	80.56	79.13	79.06	75.56	79	81.63
post-operative	72.73	71.59	70.45	71.59	69.32	67.05	70.45	72.73	69.32	68.18	69.32	68.18
primary-tumor	54.88	51.83	55.18	52.44	53.05	56.1	54.88	53.05	53.66	53.35	54.57	54.57
ringnorm	95.19	90.41	90.81	90.85	97.01	97.09	95.46	91.99	92.15	92.54	97.24	97.15
seeds	93.27	94.71	91.83	91.83	93.75	92.31	93.75	93.75	95.19	92.31	92.79	93.75
semeion	92.4	89.51	91.52	89.13	88.69	91.96	92.46	89.7	92.09	90.52	91.14	93.22
soybean	90.29	89.23	90.56	82.71	89.83	86.3	90.36	88.63	90.76	83.38	90.36	87.43
spambase	94.39	94.5	94.15	94.11	94.8	94.48	94.72	94.91	94.83	94.3	95.3	95.17
spect	68.95	61.56	65.46	59.68	60.75	61.29	65.05	60.75	63.04	60.22	61.42	62.1
spectf	91.98	91.98	91.98	91.98	91.98	91.84	91.98	91.84	91.98	91.98	91.98	91.84
statlog-australian-credit	67.3	65.26	66.57	67.15	63.66	63.23	64.39	63.37	65.55	63.52	64.53	63.08
statlog-german-credit	77.5	74.8	75.4	73.9	75.3	77.7	77.4	73.9	75.9	72.8	76.1	76.1
statlog-heart	85.45	87.31	86.19	86.19	85.45	85.45	85.07	85.82	85.45	83.21	85.45	85.45
statlog-image	97.27	97.66	97.57	96.66	97.88	97.92	97.88	97.92	98.31	97.18	98.09	98.27
statlog-landsat	89.94	89.99	89.99	89.04	89.78	89.88	90.78	90.89	90.73	89.44	90.76	90.98
statlog-shuttle	99.96	99.87	99.95	99.76	99.94	99.96	99.99	99.9	99.97	99.78	99.97	99.97
statlog-vehicle	73.58	76.3	77.73	75.95	78.08	79.03	75.71	76.18	77.61	77.25	78.32	80.45
steel-plates	78.04	78.04	76.75	75.15	75.05	76.49	78.4	78.2	78.76	76.86	77.94	77.99
synthetic-control	97.67	99.83	98.5	98.33	97.17	99.17	98.5	99.33	99.33	98.83	98.5	99.67
teaching	59.21	58.55	60.53	57.24	55.92	60.53	58.55	58.55	59.87	57.24	59.21	59.87
thyroid	98.88	95.86	98.89	93.26	98.7	97.65	98.96	96.05	98.93	93.46	98.87	98.16
tic-tac-toe	97.91	97.49	97.7	94.77	97.07	98.01	98.64	98.95	98.85	98.22	98.43	99.06
titanic	78.95	78.68	78.95	78.32	78.95	78.95	78.95	78.95	78.95	78.5	78.95	78.95
trains	87.5	100	87.5	87.5	87.5	87.5	87.5	87.5	87.5	87.5	87.5	87.5
twonorm	96.8	97.59	97.68	97.57	97.68	97.55	96.8	97.57	97.53	97.42	97.68	97.66
vertebral-column-2clases	83.77	86.69	86.04	86.04	85.06	86.69	82.14	86.36	86.36	87.01	83.44	85.06
vertebral-column-3clases	83.44	84.09	83.44	83.77	83.77	83.77	84.74	86.04	84.42	85.71	85.39	86.36
wall-following	99.3	94.24	98.41	93.71	96.17	96.19	99.52	94.54	98.57	94.68	96.87	96.92
waveform	84.54	85.4	85.04	85.44	84.8	85.4	83.76	85.26	85.9	85.48	85.12	85.78
waveform-noise	85.5	85.2	86.24	85.74	85.08	85.84	85.22	85.44	85.44	85.52	85.6	86.14
wine	97.73	98.86	99.43	97.73	97.16	98.86	97.73	97.73	99.43	98.3	97.16	99.43
wine-quality-red	65.81	68	67.38	68.19	68.31	67.56	68	67.5	69.19	67.31	68.81	67.88
wine-quality-white	67.01	67.28	67.57	66.14	67.87	67.69	68.2	67.85	67.97	66.91	68.57	68.4
yeast	61.52	62.06	61.79	62.2	62.53	62.53	60.58	61.39	61.39	60.98	60.98	61.79
zoo	99	99	98	98	99	99	98	97	98	99	98	98
Average Accuracy	81.86	81.98	81.96	80.83	81.48	81.9	82.09	81.79	82.39	80.96	82.2	82.55

[a]Denotes the methods introduced in this paper.

OM denotes oocytes_merluccius, OT denotes oocytes_trisopterus.

an ensemble, a diagram is shown as a scatter plot of $L(L-1)/2$ points with each point corresponding to a pair of classifiers being analyzed. The x-coordinate represents the diversity among the pair of base learners, also known as Kappa (κ) coefficient and the y-coordinate represents the average error of the pair of base learners. Kappa gives the level of agreement between the two base learners and while correcting for chance. For T target labels of given dataset, κ is defined on the $T \times T$ coincidence matrix C of two classifiers. Each entry in the c_{ij} represents the proportion of the testing data which one classifier predicted as kth class while the other base learner classifies it as the jth class. Kappa coefficient κ represents the level of agreement between the two

Table 3
Overall comparison of the baseline classification models, proposed oblique and rotation double random forest models.

	Rank	Average rank	Average accuracy	Average time (s)
DRaF-LDA[a]	1	5.04	82.55	758.68
MPDRaF-P[a]	2	5.45	82.39	80.83
DRaF-PCA[a]	3	5.84	82.2	765.81
RaF-LDA	4	6.12	81.9	732.63
DRaF	5	6.27	82.09	523.32
MPDRaF-T[a]	6	6.38	81.79	30.66
MPRaF-P	7	6.48	81.96	56.3
MPRaF-T	8	6.81	81.98	24.64
RaF	9	6.99	81.86	383.43
MPDRaF-N[a]	10	7.3	80.96	32.12
RaF-PCA	11	7.31	81.48	719.97
MPRaF-N	12	8	80.83	26.76

[a]Denotes the methods introduced in this paper.

Table 4
Pairwise win–tie–loss count.

	RaF	MPRaF-T	MPRaF-P	MPRaF-N	RaF-PCA	RaF-LDA	DRaF	MPDRaF-T[a]	MPDRaF-P[a]	MPDRaF-N[a]	DRaF-PCA[a]
MPRaF-T	[57, 10, 54]										
MPRaF-P	[60, 17, 44]	[60, 13, 48]									
MPRaF-N	[50, 10, 61]	[36, 14, 71]	[40, 16, 65]								
RaF-PCA	[49, 16, 56]	[51, 8, 62]	[47, 11, 63]	[63, 15, 43]							
RaF-LDA	[67, 10, 44]	[63, 10, 48]	[61, 14, 46]	[77, 13, 31]	[70, 17, 34]						
DRaF	[69, 14, 38]	[65, 8, 48]	[58, 17, 46]	[64, 11, 46]	[60, 15, 46]	[54, 11, 56]					
MPDRaF-T[a]	[56, 14, 51]	[61, 15, 45]	[54, 10, 57]	[70, 15, 36]	[60, 14, 47]	[48, 12, 61]	[52, 12, 57]				
MPDRaF-P[a]	[69, 13, 39]	[74, 10, 37]	[70, 14, 37]	[76, 12, 33]	[68, 18, 35]	[67, 9, 45]	[63, 16, 42]	[59, 16, 46]			
MPDRaF-N[a]	[46, 14, 61]	[44, 12, 65]	[45, 13, 63]	[74, 13, 34]	[55, 14, 52]	[40, 12, 69]	[47, 14, 60]	[36, 17, 68]	[37, 13, 71]		
DRaF-PCA[a]	[61, 14, 46]	[65, 10, 46]	[56, 16, 49]	[77, 11, 33]	[72, 22, 27]	[64, 14, 43]	[57, 14, 50]	[59, 10, 52]	[49, 20, 52]	[70, 11, 40]	
DRaF-LDA[a]	[69, 11, 41]	[70, 10, 41]	[62, 15, 44]	[79, 11, 31]	[71, 16, 34]	[77, 12, 32]	[67, 12, 42]	[68, 15, 38]	[62, 13, 46]	[79, 8, 34]	[66, 22, 33]

[a]Denotes the proposed methods, $[a, b, c]$ entry in each cell denotes that row method wins a-times, loses c-times and ties b-times with respect to column method.

Table 5
Pairwise win–tie–loss: Sign test.

	RaF	MPRaF-T	MPRaF-P	MPRaF-N	RaF-PCA	RaF-LDA	DRaF	MPDRaF-T[a]	MPDRaF-P[a]	MPDRaF-N[a]	DRaF-PCA[a]	DRaF-LDA[a]
RaF						$r-$	$r-$		$r-$			$r-$
MPRaF-T									$r-$			$r-$
MPRaF-P									$r-$			
MPRaF-N						$r-$		$r-$	$r-$	$r-$	$r-$	$r-$
RaF-PCA						$r-$			$r-$		$r-$	$r-$
RaF-LDA	$r+$			$r+$	$r+$				$r-$			$r-$
DRaF	$r+$											$r-$
MPDRaF-T[a]				$r+$								$r-$
MPDRaF-P[a]	$r+$	$r+$	$r+$	$r+$	$r+$	$r+$						
MPDRaF-N[a]				$r+$							$r-$	$r-$
DRaF-PCA[a]				$r+$	$r+$					$r+$		$r-$
DRaF-LDA[a]	$r+$	$r+$		$r+$	$r+$	$r+$	$r+$	$r+$		$r+$	$r+$	

[a]Denotes the methods introduced in this paper, $r+$ denotes that the method in the corresponding row is significantly better as compared to the method given in the corresponding column. $r-$ denotes that the row method is significantly worse than the method given in the corresponding column. Blank entries denote that no significant difference exists among the methods in the cell's corresponding row and column.

Table 6
Average rank of the classification models with different *minleaf* parameters.

Method	*minleaf* $= 1$	*minleaf* $= 2$	*minleaf* $= 3$	F_F
RaF	1.87	1.87	2.26	6.3555
MPRaF-T	1.79	1.93	2.29	11.2753
MPRaF-P	1.66	2.11	2.23	11.8124
MPRaF-N	1.73	1.95	2.32	11.6113
RaF-PCA	1.73	2.01	2.27	12.1945
RaF-LDA	1.77	2.01	2.22	6.3555
DRaF	1.65	2.08	2.27	13.3546
MPDRaF-T*	1.87	1.94	2.19	3.4658
MPDRaF-P*	1.74	1.98	2.28	9.3988
MPDRaF-N*	1.76	1.93	2.3	7.0927
DRaF-PCA*	1.68	2	2.32	13.5758
DRaF-LDA*	1.8	2.08	2.11	1.111

classifiers and is given as follows:

$$\kappa = \frac{p_r(a) - p_r(e)}{1 - p_r(e)} \tag{14}$$

where $p_r(a)$ is the observed agreement between the two classifiers i.e. probability that both classifiers predicted the same label and the $p_r(e)$ is the hypothetical probability of agreement by

(a) Echocardiogram

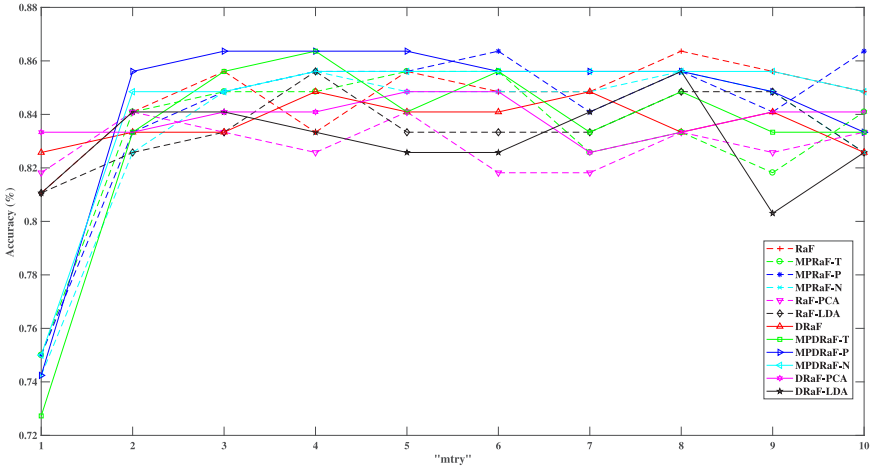

(b) Ecoli

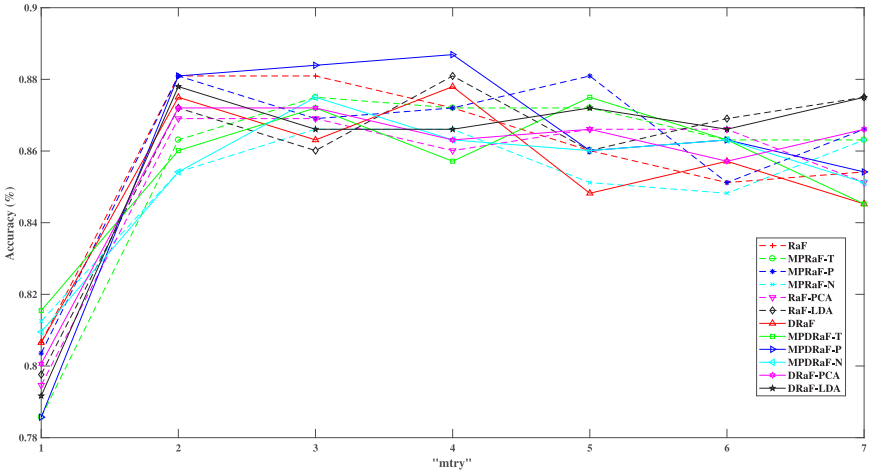

(c) Soybean

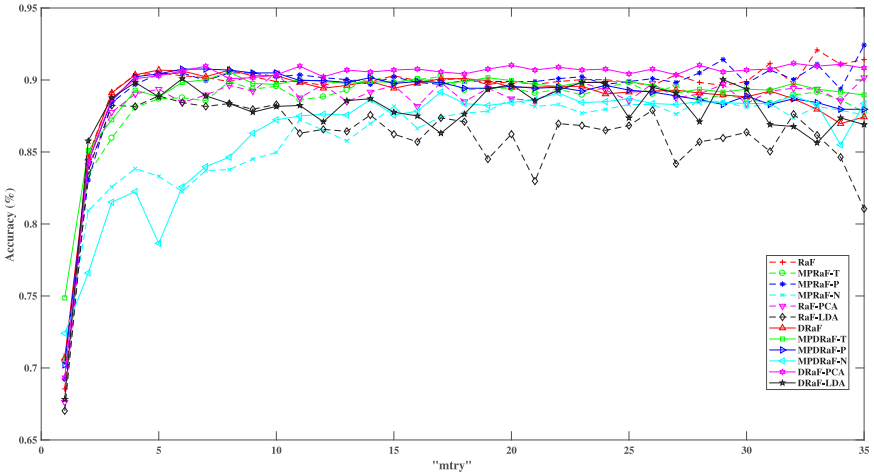

Fig. 2. Effect of the "*mtry*" parameter.

chance. Mathematically,

$$p_r(a) = \sum_i c_{ii}, \tag{15}$$

$$p_r(e) = \sum_k \left[\left(\sum_i m_{ki} \right) \left(\sum_j m_{jk} \right) \right]. \tag{16}$$

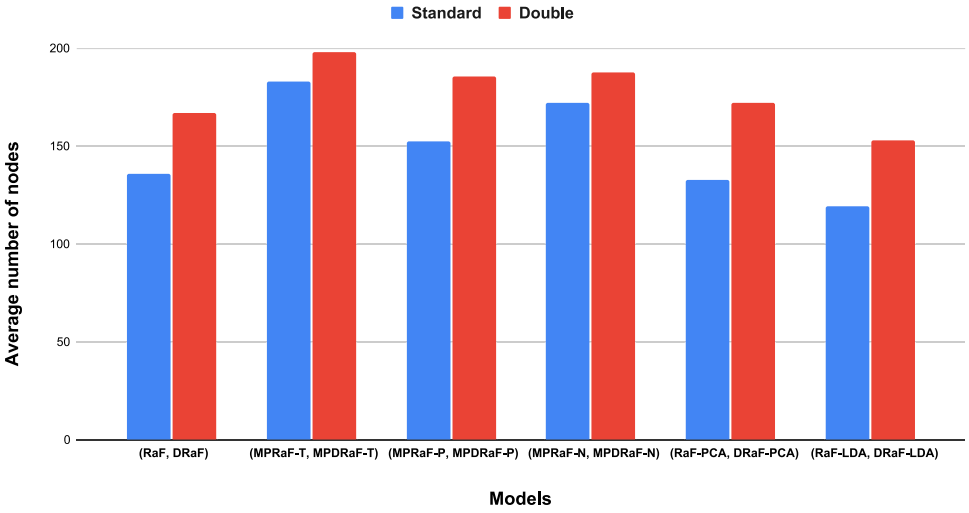

Fig. 3. Mean node analysis.

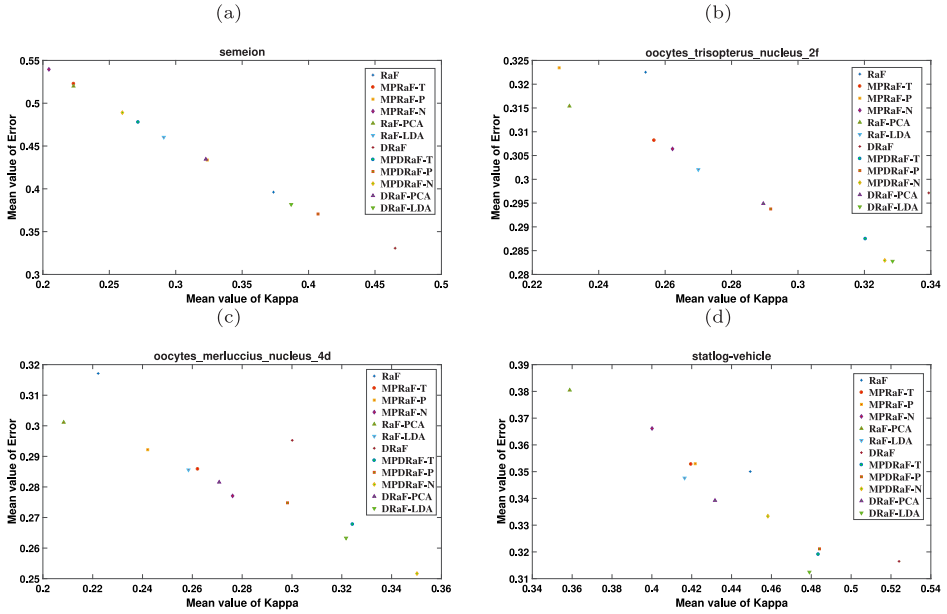

Fig. 4. Centroid of Kappa error diagrams on different datasets.

If the two decision trees are in complete agreement, then the kappa coefficient (κ) is 1 and the two trees are identical. If the trees are independent, then the kappa coefficient (κ) is 0. As mentioned above, we evaluate $L(L-1)/2$ pairs of kappa coefficients. Also, averaged error of the individual classifiers $E_{i,j} = (E_i + E_j)/2$. The smaller κ value indicates better diversity or low correlation while as the smaller averaged error E represents the more accurate or better strength classifier. The most desirable pair of classifiers is the one in the bottom left corner of Fig. 4.

Fig. 4 plots the kappa error diagram for some datasets. Figure 1, 2, 3 and 4 of the supplementary file shows the kappa error diagram for the semeion, oocytes_trisopterus_nucleus_2f, oocytes_merluccius_nucleus_4d and statlog-vehicle datasets. The ensemble size is 50, hence, 1225 dots in each plot. Figure 1(a) to Figure 1(l) of the supplementary file show the kappa error diagrams of the classification models on different datasets. All the classification models are trained on the training data samples and κ-error diagrams are plotted based on the performance of the classification models on the testing samples (in some diagrams the axis are adjusted for better view).

Fig. 4 represents the centroid of the scatter points for each classification model corresponding to the semeion, oocytes_merluccius_nucleus_4d, oocytes_trisopterus_nucleus_2f and statlog-vehicle datasets. From the given plots, different models of the random forest possess different characteristics. Fig. 4(a) plot shows that MPRaF-N is the most diverse classifier (least mean value of kappa) and DRaF is the most accurate classifier (least mean value of error). However, DRaF-LDA ensemble classifiers possess the best overall generalization performance on this dataset. From the plot, one can see that the proposed DRaF-LDA have the better combination of diversity and error. Similarly in other datasets, the models with better combination results in better performance.

7. Analysis of computational complexity

Here, we evaluate the computational complexity of the classifiers. Without assuming any structure of decision trees, we focus on the complexity involved at a given node. Let a given node receives m number of samples with n number of features. In axis

Table 7
Average number of nodes in RaF (Breiman, 2001), MPRaF-T (Zhang & Suganthan, 2014a), MPRaF-P (Zhang & Suganthan, 2014a), MPRaF-N (Zhang & Suganthan, 2014a), RaF-PCA (Zhang & Suganthan, 2014b), RaF-LDA (Zhang & Suganthan, 2014b), DRaF (Han et al., 2020), MPDRaF-Tf, MPDRaF-P, MPDRaF-N, DRaF-PCA AND DRaF-LDA classification models.

Datasets	RaF	MPRaF-T	MPRaF-P	MPRaF-N	RaF-PCA	RaF-LDA	DRaF	MPDRaF-T*	MPDRaF-P*	MPDRaF-N*	DRaF-PCA*	DRaF-LDA*
abalone	349.81	481.93	392.75	372.79	304.43	296.08	470.07	447.08	491.77	324.92	444.69	439.34
acute-inflammation	4.9	5.04	4.97	4.74	4.46	4.44	5.05	4.99	5.18	4.72	4.32	4.54
acute-nephritis	3.89	4.46	4.03	4.09	3.57	3.66	4.01	4.48	4.3	4.27	3.52	3.77
adult	1731.66	2113.55	1843.9	1846.68	1480.15	1489.83	2132.73	2456.92	2321.47	2021.68	2016.47	1965.98
annealing	34.1	55.84	34.65	46.51	32.62	34.05	40.54	68.02	40.73	54.3	38.96	40.03
arrhythmia	36.6	63.65	36.12	63.92	34.81	35.39	43.64	58.73	43.54	58.12	46.24	47.53
audiology-std	17.26	23.98	17.22	23.18	16.63	17.89	14.43	26.65	13.98	23.34	15.89	16.14
balance-scale	38.45	38.18	37.65	34.35	32.13	30.73	35.96	36.71	36.53	30.1	33.8	32.89
balloons	2.1	1.84	2.13	1.78	2.23	2.33	1.25	1.28	1.38	1.32	1.92	1.86
bank	167.83	245.75	185.29	218.47	140.31	138.89	232.43	294.41	250.61	264.36	207.68	203.55
blood	44.22	39.85	47.36	44.86	41.17	40.84	54.81	41.74	54.41	46.77	56.34	56.92
breast-cancer	26.38	28.39	26.35	26.41	21.9	21.39	29.49	31.43	31.22	26.8	31.53	28.97
breast-cancer-wisc	14.94	17.11	14.83	17.75	11.36	10.34	19.77	19.92	18.68	22.86	16.07	15.21
breast-cancer-wisc-diag	11.41	14.47	11.79	18.57	11.87	8.36	16.65	18.06	15.71	23.04	17.41	11.69
breast-cancer-wisc-prog	12.66	17.26	13.81	19.59	11.65	9.77	19.42	21.51	20.14	23.98	19.2	17.14
breast-tissue	10.22	13.94	11.58	12.88	10.03	9.45	12.42	11.86	13.4	9.65	12.85	12.45
car	52.05	53.99	59.95	38.74	56.29	51.94	48.68	51.09	57.2	32.38	55.22	51.35
cardiotocography-10clases	134.08	242.91	144.6	253.69	134.46	113.43	161.43	256.29	174.09	270.15	176.92	148.62
cardiotocography-3clases	63.94	110.23	71.05	122.75	60.33	54.43	80.75	127.33	90.16	144.95	85.3	75.46
chess-krvk	922.92	1341.55	1138.44	651.32	1250.65	1226.39	720.29	897.58	876.76	390.42	1014.06	982.35
chess-krvkp	91.09	158.26	96.72	130.73	94.32	90.97	98.88	190.97	106.51	149.3	110.76	102.34
congressional-voting	9.03	11.01	8.65	8.95	8.6	8.12	6.46	13.07	6.49	10.67	8.65	8.58
conn-bench-sonar-mines-rocks	11.95	17.62	12.94	19.71	11.59	8.2	19.3	21.92	21.08	24.68	19.88	15.11
conn-bench-vowel-deterding	61.24	92.06	71.79	94.91	58.61	52.83	77.37	103.21	89.43	94.97	76.15	67.79
connect-4	1967.07	2058.1	1891.47	1183.77	2060.35	2069.17	2042.64	2231.71	1938.48	1325.44	2340.46	2169.71
contrac	132.21	143.02	134.2	112.51	122.42	118.87	131.37	124.59	137.45	94	144.96	138.52
credit-approval	38.91	57.35	43.62	52.44	34.06	32.43	52.69	67.08	56.72	61.46	51.09	47.16
cylinder-bands	41.29	57.62	42.98	58.21	32.63	30.92	59.68	63.21	63.02	63.14	52.22	51.39
dermatology	16.57	21.36	16.72	22.93	15.93	15.07	18.75	25.76	18.88	26.48	18.59	19.01
echocardiogram	9.39	12.91	10.54	13.51	8.47	8.16	12.5	13.4	13.18	13.64	12.37	11.55
ecoli	21.06	29.67	22.12	29.22	19.55	19.53	24.27	30.18	25.9	29.94	24.87	24.44
energy-y1	19.81	28.57	21.12	23.27	21.05	19.8	20.84	28.92	22.49	22.94	22.88	20.51
energy-y2	20.16	27.39	21.02	21.62	19.94	18.93	19.06	26.41	19.82	19.59	20.55	20.12
fertility	6.59	7.89	6.98	7.71	5.3	4.98	7.55	8.45	7.9	8.06	6.39	6.25
flags	22.14	29.94	23.32	30.2	19.74	19.1	20.38	24.02	20.65	23.11	22.19	22.11
glass	19.94	28.3	20.21	27.43	18.29	17.5	23.35	26.87	24.81	24.85	24.46	24.13
haberman-survival	25.08	30.43	27.5	30.54	22.39	22.72	31.43	30.7	29.78	29.58	31.97	31.9
hayes-roth	9.48	11.65	10.47	11.06	9.27	9.57	9.25	12.94	10.4	12.14	9.38	10.1
heart-cleveland	29.28	38.23	30.57	38.94	24.89	23.78	31.77	30.35	31.28	31.75	32.14	31.8
heart-hungarian	19.39	24.65	20.9	22.62	17.24	16.58	23.73	27.59	25.09	23.16	24.27	22.77
heart-switzerland	16.19	18.03	15.94	16.19	13.97	14.5	13.85	11.5	14.31	10.72	15.2	15
heart-va	24.8	29.49	24.4	25.87	22.4	22.69	21.02	17.98	21.08	16.34	25.44	25.66
hepatitis	10.18	13.48	10.88	12.77	8.45	7.74	13.07	14.49	13.59	13.81	11.91	11.54
hill-valley	66.19	35.12	78.26	66.38	44.66	33.52	107.02	48.96	113.11	81.06	71.38	57.43
horse-colic	24.01	35.35	26.48	36.79	21.26	18.99	30.83	42.35	35.99	43.91	32.1	29.08
ilpd-indian-liver	42.55	62.23	52.69	59.59	37.81	36.36	64.22	66.84	70.02	61.38	60.39	60.05
image-segmentation	15.59	27.32	18.32	28.83	15.1	13.31	18.55	29.1	22.34	31.26	19.57	17.15
ionosphere	13.52	21.57	16.08	23.27	12.08	10.21	18.44	27.29	22.89	29.9	18.13	15.86
iris	5.29	7.04	5.75	6.28	5.98	4.31	5.84	6.99	6.15	6.31	7.45	5.29
led-display	12.41	13.45	12.54	12.22	13.08	13.42	10.19	11.76	9.96	9.72	11.3	10.27
lenses	2.8	2.61	2.75	2.78	2.78	2.77	2.15	1.85	2.01	2.12	2.19	2.29
letter	1190.77	1941.31	1545.76	2019.17	1105.98	930.41	1277.75	1958.65	1592.73	1954.44	1307.54	1096.94
libras	35.05	52.7	41.16	56.74	33.61	24.04	46.59	58.94	50.94	60.77	45.32	35.67
low-res-spect	21.64	30.63	24.64	41.84	22.72	15.78	29.46	37.97	32.4	54.2	29.92	22.45
lung-cancer	4.49	4.47	4.37	4.87	4.04	3.63	4.23	3.11	4.42	3.11	4.3	4.2
lymphography	13.44	16.54	12.94	16.01	10.45	10.4	15.29	17.56	15.17	16.81	14.91	13.9
magic	778.89	1291.33	1027.86	1307.15	753.48	712.13	1111.39	1482.07	1405	1449.84	1107.32	1065.07
mammographic	44.23	41.93	46.28	37.9	38.79	40.24	55.53	50.51	55.49	44.05	51.62	52.76
miniboone	2878.18	3186	3325.18	3415.87	2829.45	2159.2	4173.28	3917.6	4949.34	4402.77	4223.4	3380.49
molec-biol-promoter	8.25	11.47	9.13	11.27	7.16	5.22	11.85	12.52	12.61	12.61	12.22	9.04
molec-biol-splice	176.93	313.37	203.18	340.19	189.1	121.92	222.68	344.12	267.96	367.3	270.48	185.86
monks-1	13.76	14.75	14.34	13.17	13.46	13.17	13.82	14.26	14.8	12.42	14.68	14.39
monks-2	18.58	19.18	19.15	17.15	19.37	20.08	17.63	15.94	17.98	13.79	21.23	20.87
monks-3	11.2	12.73	12.65	11.99	10.42	10.54	12.02	12.08	12.44	11.3	11.67	11.34
mushroom	22.75	40.82	28.52	40.07	25.59	22.62	22.69	41.7	29.31	40.72	25.97	22.32
musk-1	24.84	38.13	27.21	42.76	23.55	14.11	38.03	49.24	42.81	56.82	39.26	25.85
musk-2	122.19	209.28	154.56	269.33	131.13	80.8	155.73	272.22	218.71	358.09	185.13	119.86
nursery	251.01	304.95	292.95	227.6	284.02	229	238.47	317.62	291.65	207.74	284.79	238.4
OM_nucleus_4d	60.42	82	67.16	77.37	49.74	41.21	90.32	96.09	97.68	97.48	78.41	65.48
OM_states_2f	28.9	43.9	34.34	50.86	29.16	22.92	41.53	54.12	47.79	63.07	41.68	34.74
OT_nucleus_2f	54.49	81	67.18	87.08	49.45	43.09	81.65	97.52	96.57	105.17	78.13	69.05

(*continued on next page*)

Table 7 (*continued*).

Datasets	RaF	MPRaF-T	MPRaF-P	MPRaF-N	RaF-PCA	RaF-LDA	DRaF	MPDRaF-T*	MPDRaF-P*	MPDRaF-N*	DRaF-PCA*	DRaF-LDA*
OT_states_5b	35.15	48.35	36.61	60.54	32.36	24.35	50.86	61.42	54.25	80.15	47.17	36.41
optical	210.94	383.82	219.43	467.41	204.48	183.58	244.67	454.88	253.86	562.79	246.3	218.09
ozone	28.65	41.55	31.06	52.34	27.68	20.37	42.9	56.45	45.01	74.71	40.87	31.9
page-blocks	63.65	91.79	72.87	85.22	59.51	59	78.39	102.96	92.8	89.51	77.12	77.25
parkinsons	8.53	12.85	10.47	13.85	8.53	7.28	12.53	15.65	14.38	16.36	12.63	10.9
pendigits	210.57	320.17	237.25	385.79	200.55	153.25	254.88	371.52	279.76	434.7	245.63	188.28
pima	49.77	73.48	61.52	77.61	45.37	43.15	71.98	79.12	81.43	81.48	71.59	69
pittsburg-bridges-MATERIAL	7.64	8.8	7.63	8.55	6.54	6.35	8.78	9.04	8.5	8.33	7.39	7.36
pittsburg-bridges-REL-L	11.41	12.56	11.42	12.48	9.7	9.55	11.93	12.62	12.23	11.47	11.32	10.99
pittsburg-bridges-SPAN	10.1	11.39	10.42	11.4	8.78	8.55	10.38	10.78	10.49	9.89	9.76	9.72
pittsburg-bridges-T-OR-D	6.56	7.48	6.65	7.78	5.28	4.93	7.27	8.55	7.66	8.49	6.45	5.95
pittsburg-bridges-TYPE	12.21	14.65	12.47	14.11	11.06	11.04	11.24	11.1	11.46	11.3	10.85	10.98
planning	14.76	21.19	18.04	22.72	14.07	13.81	22.81	22.24	24.48	22.64	22.64	22.4
plant-margin	185.17	278.12	226.79	284.17	177.44	162.35	208.88	237.69	224.82	215.9	214.61	198.11
plant-shape	179.46	269.87	225.2	266.63	172.3	151.38	211.7	223.83	224.9	208.34	211.32	185.95
plant-texture	183.56	280.18	229.79	288.43	185.23	174.11	204.49	239.06	224.63	228.76	213.6	203.7
post-operative	9.47	10.15	9.36	9.94	8.33	8.2	8.78	9.8	9.02	8.52	9.1	8.89
primary-tumor	30.61	35.14	30.93	29.84	29.14	27.48	28.67	28.18	27.73	25.73	26.43	23.9
ringnorm	192.09	94.06	78.06	97.7	184.54	177.42	278.44	94.96	81.93	106.52	276.47	270.66
seeds	7.75	9.65	8.57	9.61	7.46	5.71	10.24	10.99	10.03	10.33	9.25	7.65
semeion	133.92	200.29	140.83	211.13	112.95	74.38	134.27	205.83	142.29	217.42	129.69	95.45
soybean	34.87	43.67	34.94	42.07	31.01	30.76	38.45	48.22	38.59	46.51	35.89	34.99
spambase	145.86	266.25	155.26	264.33	126.5	128.33	185.34	359.57	195.29	330.51	172.87	172.18
spect	8.87	10.66	9.01	10.16	7.56	7.34	7.92	11.14	8.36	9.83	9.03	8.89
spectf	7.22	9.79	7.9	8.53	6.88	5.17	10.53	12.95	11.62	11.17	11.03	8.53
statlog-australian-credit	61.65	84.09	67.34	80.9	51.56	50.41	88.45	86.61	93.81	81.66	82.81	81.69
statlog-german-credit	83.54	104.95	86.89	98.17	62.34	61.28	114.18	115.94	116.87	111.89	96.46	93.76
statlog-heart	19.09	23.63	19.61	24.06	15.01	13.64	25.98	27	25.5	27.88	22.85	21.07
statlog-image	53.56	104.54	66.08	110.84	55.86	44.66	64.94	122.42	82.5	126.87	70.88	57.08
statlog-landsat	212.51	282.05	215.65	348.32	183.51	147.53	279.69	349.92	291.84	441.74	255.52	214.28
statlog-shuttle	43.13	85.75	50.42	88.78	50.5	46.36	46.61	96.3	55.25	92.36	56.93	53.09
statlog-vehicle	62.92	86.28	69.01	86.57	54.83	48.37	84.86	88.85	89.87	86.25	80.76	72.17
steel-plates	137.59	219.51	151.26	223.54	127.45	116.3	174.26	212	191.89	216.55	172.86	163.19
synthetic-control	22.45	30.57	24.67	47.6	22.3	14.81	31.6	39.99	33.12	68.44	31.62	23.2
teaching	16.53	15.55	15.79	13.96	14.67	15.2	17.06	13.03	16.26	10.53	16.72	16.82
thyroid	35.33	97.28	38.4	86.65	43.65	40.25	40.6	125.71	41.32	102.93	53.44	49.49
tic-tac-toe	63.59	74.08	68.68	70.4	53.15	49.43	69.82	89.25	79.65	78.96	68.94	60.88
titanic	2.11	1.79	1.96	1.22	1.89	1.92	1.78	1.57	1.67	1.02	1.66	1.58
trains	1.86	1.83	1.82	1.84	1.85	1.87	1.86	1.33	1.83	1.29	1.62	1.79
twonorm	228.12	218.97	174.37	246.81	148.81	117.17	338.36	276.83	242.89	304.57	213.91	179.02
vertebral-column-2clases	16.76	24.45	21.93	22.62	17.19	16.12	23.89	26.32	26.1	24.54	24.36	23.27
vertebral-column-3clases	17.79	27.44	22.68	23.81	19.01	17.86	24.66	27.57	27	25.11	26.38	24.15
wall-following	75.12	447.26	206.66	457	200.73	172.75	87.98	525.26	292.24	542.77	260.06	226.96
waveform	235.29	341.47	263.81	393.89	218.79	171.81	345.63	422.09	393.9	497.19	334.64	274.58
waveform-noise	248.63	394.91	283.88	450.01	252.12	178.42	364.23	477.08	430.04	541.41	371.84	285.08
wine	6.59	8.7	7.12	11.46	6.78	5.45	8.63	10.95	8.85	12.68	9.05	7.46
wine-quality-red	145.57	216.6	160.1	214.39	129.81	128.37	187.58	205.59	199.63	196.07	182.78	180.84
wine-quality-white	469.5	680.6	513.65	660.92	417.41	409.4	596.95	643.95	635.97	596.16	573.59	569.44
yeast	154.13	205.48	159.04	180.27	139.59	140.98	173.4	158.29	176.88	145.17	175.34	176.23
zoo	7.05	8.55	7.22	8.02	6.7	6.63	7.21	9	7.41	8.29	7.29	7.32
Average of Mean Nodes	135.98	183.01	152.44	172.21	132.99	119.17	166.91	198.03	185.75	187.43	171.87	153.07

Here, OM denotes oocytes_merluccius, OT denotes oocytes_trisopterus.

parallel splits, the optimum threshold is chosen based on some impurity criteria via ranking of each feature. Despite the complexity of the gini impurity, the complexity of the search involved in optimal split is $O(nm\ \log\ m)$ (Zhang & Suganthan, 2014a). For MPSVM based oblique decision trees, the computational complexity of generalized problem is $O(n^3)$ (Manwani & Sastry, 2011). In decision trees wherein the feature transformations (PCA and LDA) are used for projecting the input features, additional computational time is involved for calculating the projection matrix. The complexity of the PCA is $O(mn \times \min(m, n) + n^3)$ (Kreßner, 2004) while as for LDA the complexity is $O(mn^2)$ (Chu et al., 2007). MPSVM based decision tree ensembles are faster as compared to the standard ensemble models. The reason is that in most of the cases, particularly for the nodes near the root, MPSVM method is faster compared to the exhaustive search. The training time of the proposed DRaF-PCA and DRaF-LDA is more as compared to the RaF-PCA and RaF-LDA, respectively, due to the reason that the bootstrapping at each non-leaf node of the proposed DRaF-PCA and DRaF-LDA leads to more number of unique samples to be sent down the tree resulting in more deeper decision trees. The average training time of each classification model is given in Table 3. The training time of the classification models on each dataset is given in Table 2 of the supplementary file.

8. Bias–variance analysis

In this section, we discuss the bias–variance analysis of the ensemble models. Bias–variance analysis is the main reason for the success of ensemble models. The concept of bias–variance is well known in the regression problems for the squared loss functions (Geman, Bienenstock, & Doursat, 1992). However, this analysis is inappropriate as the labels of the classes are categorical. Thus, it is not feasible to transplant the decomposition of error in regression problems to classification problems. In classification problems, several studies have provided the ways to decompose the classification error into bias–variance terms (Friedman, 1997; James, 2003; Kong & Dietterich, 1995). Each of these studies provide some insight into the models performance.

Table 8
Bias–variance analysis of RaF (Breiman, 2001), MPRaF-T (Zhang & Suganthan, 2014a), MPRaF-P (Zhang & Suganthan, 2014a), MPRaF-N (Zhang & Suganthan, 2014a), RaF-PCA (Zhang & Suganthan, 2014b), RaF-LDA (Zhang & Suganthan, 2014b), DRaF (Han et al., 2020), MPDRaF-T, MPDRaF-P, MPDRaF-N, DRaF-PCA and DRaF-LDA classification models.

Datasets	RaF Bias Variance	MPRaF-T Bias Variance	MPRaF-P Bias Variance	MPRaF-N Bias Variance	RaF-PCA Bias Variance	RaF-LDA Bias Variance	DRaF Bias Variance	MPDRaF-T* Bias Variance	MPDRaF-P* Bias Variance	MPDRaF-N* Bias Variance	DRaF-PCA* Bias Variance	DRaF-LDA* Bias Variance
abalone	422.19	421.95	422.16	409.26	424.42	420.62	415.77	411.11	417.33	399.97	415.42	413.34
	220.38	224.11	226.61	206.18	228.12	225.96	202.89	204.21	214.17	190.48	215.17	214.64
acute-inflammation	2.21	1.48	2.14	1.99	1.72	1.74	1.81	1.44	1.64	2.07	1.56	1.53
	1.84	1.31	1.84	1.74	1.52	1.48	1.53	1.25	1.4	1.83	1.31	1.32
acute-nephritis	1.14	0.86	1.14	1.53	0.74	0.72	0.53	0.86	0.71	1.18	0.58	0.53
	0.99	0.8	1.02	1.41	0.66	0.66	0.49	0.8	0.66	1.09	0.54	0.5
adult	3032.87	3261.33	3192.13	3669.3	3341.57	3802.34	2798.83	2993.5	2967.71	3432.11	3175.48	3539.3
	1423.89	1552.82	1555.3	1908.44	1718.95	2123.73	1110.31	1241.92	1287.36	1646.2	1553.7	1886.05
annealing	56.94	76.64	54.6	80.44	62.27	63.7	52.45	78.1	58.66	80.84	63.66	64.95
	24.71	23.7	25.63	21.81	33.16	34.4	23.87	21.74	24.56	22.91	32.91	34.78
arrhythmia	48.16	55.61	47.75	54.86	53.39	53.65	45.18	52.32	45.5	50.95	49.35	50.5
	30.55	35.78	30.37	35.2	34.99	35.65	26.16	30.44	26.79	28.58	29.82	32.12
audiology-std	11.27	14.81	10.96	15.59	15.04	14.59	11	14.25	11.12	15.71	14.47	14.25
	6.9	10.19	6.73	10.3	10.22	9.98	5.79	9.92	6	10.03	9.82	9.83
balance-scale	34.84	30.63	31.25	30.69	32.12	30.29	32.76	28.41	28.69	27.46	30.59	27.93
	22.44	20.42	20.46	20.4	21.08	19.99	17.75	17.64	17.18	16.99	17.8	16.84
balloons	1.42	1.42	1.41	1.35	1.43	1.33	1.26	1.19	1.27	1.31	1.11	1.14
	0.8	0.82	0.82	0.83	0.84	0.77	0.66	0.67	0.65	0.75	0.65	0.66
bank	158.45	171.54	164.99	165.29	168.34	166.13	146.42	151.74	152.84	148.85	155.18	153.4
	79.65	85.26	83.55	76.1	87.21	84.7	67.42	64.8	70.35	59.45	75	73.58
blood	52.18	50.54	51.52	50.64	52.67	52.28	47.96	44.88	48.01	46.45	49.84	49.51
	19.29	18.11	19.18	19.06	19.8	19.75	11.12	10.79	11.85	12.1	13.16	12.94
breast-cancer	24.34	24.42	24.36	23.73	24.75	24.51	21.58	22.02	21.87	20.98	22.56	22.05
	11.77	11.85	11.78	11.64	12.35	12.23	8.8	9.28	9	8.51	9.87	9.6
breast-cancer-wisc	9.94	9.37	8.91	9.06	9.99	9.29	9.31	8.12	8.07	8.01	8.91	8.75
	5.92	5.6	5.22	4.98	6.03	5.35	5.25	4.5	4.5	4.38	4.99	4.89
breast-cancer-wisc-diag	11.58	9.6	10.32	10.57	13.13	10.09	10.13	8.5	8.84	8.47	11.23	8.46
	6.82	5.79	6.28	6.57	8.5	6.47	5.65	4.93	5.16	4.91	7.17	5.07
breast-cancer-wisc-prog	16.76	15.82	16.42	16.32	17.21	16.64	15.98	14.64	15.08	14.58	15.74	16.16
	8.9	8.65	8.63	8.73	9.24	8.94	8.11	7.55	7.98	7.41	8.29	8.43
breast-tissue	9.3	9.45	9.77	9.95	10.14	9.38	8.33	9.1	8.89	9.2	8.96	8.71
	5.28	5.81	5.84	6.32	6.47	5.91	4.45	4.87	4.85	5.37	5.18	4.9
car	53.62	66.26	57.3	82.54	57.16	51.75	47.24	60.48	48.71	76.95	46.33	42.38
	40.16	49.16	43.61	52.95	43.64	39.4	35.52	44.72	37.55	46.94	35.5	33.03
cardiotocography-10clases	131.33	173.39	137.05	184.31	167.74	146.51	109.53	152.42	116.46	171.16	142.7	125.47
	89.8	125.16	96.6	132.33	124.55	106.39	70.11	106.29	76.81	121.06	102.89	86.74
cardiotocography-3clases	57.33	73.66	62.12	78.34	73.06	69.02	47.51	62.48	51.28	68.54	62.08	57.57
	37.12	47.85	40.8	50.63	47.74	45.32	28.08	38.44	31.89	42.3	38.38	36.22
chess-krvk	3034.05	3362.72	3124.59	3727.55	2940.16	2994.79	2827.31	3183.27	2887.18	3648.43	2662.02	2724.99
	2059.91	2326.91	2178.24	2416.27	2080.07	2093.71	1831.25	2132.02	1957.51	2302.68	1831.15	1848.16
chess-krvkp	80.61	120.16	83.73	155.37	102.15	90.43	58.94	98.25	64.73	138.61	79.92	73.46
	61.57	90.21	64.48	113.06	77.99	69.75	44.63	74.42	50.15	102.97	61.82	57.61
congressional-voting	44.37	44.87	45.13	44.68	46.33	45.13	42.7	42.79	42.63	43.49	43.21	42.87
	16.03	14.65	15.34	13.96	18.56	17.31	3.25	3.8	3.4	6.23	5.88	4.65
conn-bench-sonar-mines-rocks	17.83	17.62	18.6	18	19.54	17.24	16.33	16.47	16.78	16.82	17.18	15.5
	10.12	10.15	10.55	10.38	11.02	9.62	9.37	9.19	9.77	9.4	9.89	8.92
conn-bench-vowel-deterding	116.57	95.58	112.38	124.23	121.65	109.1	76.15	60.54	70.67	101.47	78.76	68.95
	105.4	92.13	105.05	117.06	113.98	102.3	71.13	61.26	69.17	99.09	78.68	68.13
connect-4	3786.62	4350.55	3949.26	4354.23	4067.8	3991.2	3372.93	4027.03	3573.11	4160.29	3628	3581.14
	1936.33	1787.5	1932.43	1384.57	2150.1	2055.04	1546.41	1353.85	1556.88	1148.35	1772.59	1673.69
contrac	178	186.21	182.14	187	181.85	181.28	175.47	182.93	178.55	180.44	179.98	179.21
	91.6	96.67	94.68	98.58	94.61	93.99	75.21	82	80.1	87.81	80.62	80.66
credit-approval	35.78	38.42	38.92	37.32	39.4	38.34	33.89	34.78	34.9	35.15	37.12	35.42
	19.87	21.82	22.12	20.93	22.69	21.69	17.87	17.97	19.05	18.67	20.57	19.26
cylinder-bands	44.55	49.18	46.05	48.93	47.79	46.45	40.46	47.67	42.35	46.89	44.39	43.68
	25.53	27.29	26.23	26.87	27.08	26.09	23.47	26.66	24.57	26.55	25.48	24.91
dermatology	9.98	10.83	9.38	11.47	13.46	11.9	7.52	9.16	7.64	9.71	10.38	9.35
	8.43	9.44	7.97	9.97	11.84	10.41	5.96	7.71	6.03	8.33	9.03	8.01
echocardiogram	9.15	8.86	9.1	9.38	9.44	9.19	8.03	7.87	8.28	8.04	8.78	8.11
	4.68	4.69	4.87	4.96	5.04	4.95	3.72	3.77	4.15	3.79	4.38	4.03
ecoli	18.23	19.64	18.28	20.9	19.4	18.85	15.41	17.79	15.86	19.05	16.9	16.7
	10.84	11.67	10.89	13.62	12.08	11.52	7.47	9.45	8.21	11.62	8.97	8.87
energy-y1	16.04	24.28	17.47	23.22	20.83	17.95	12.73	19.82	13.21	20.27	15.18	13.49
	8.06	14.04	9.48	13.82	12.6	10.71	5.35	9.79	5.86	10.98	8.25	7.04

(*continued on next page*)

Table 8 (*continued*).

Datasets	RaF	MPRaF-T	MPRaF-P	MPRaF-N	RaF-PCA	RaF-LDA	DRaF	MPDRaF-T*	MPDRaF-P*	MPDRaF-N*	DRaF-PCA*	DRaF-LDA*
	Bias	Bias	Bias	Bias	Bias	Bias	Bias	Bias	Bias	Bias	Bias	Bias
	Variance	Variance	Variance	Variance	Variance	Variance	Variance	Variance	Variance	Variance	Variance	Variance
energy-y2	23.08	26.22	23.5	27.07	24.83	23.9	22.61	23.18	21.97	26.04	23.07	22.62
	10.96	13.58	11.08	14.46	12.98	12.13	7.2	9.18	7.58	12.87	9.78	8.9
fertility	4.31	4.93	4.55	4.56	4.73	4.57	3.67	3.86	3.91	3.7	3.9	3.95
	1.94	2.47	2.06	2.06	2.27	2.09	1.12	1.31	1.38	1.08	1.43	1.47
flags	21.28	25.33	22.76	25.36	24.8	25	19.63	24.64	20.77	24.74	23.38	23.12
	14.72	16.74	15.71	17.01	16.75	17.04	12.68	15.6	13.78	15.65	15.34	15.29
glass	19.46	20.25	19.09	20.78	20.5	20.51	16.67	18.63	17.23	19.99	18.63	18.57
	12.45	12.55	12.2	12.87	13.1	12.98	9.7	10.73	10.14	11.45	11.37	11.18
haberman-survival	25.47	25.79	25.48	25.05	26.5	26.28	25.04	24.18	24.92	24.09	25.51	25.24
	11.01	11.38	11	10.92	11.64	11.61	7.83	8.31	8.69	8.14	8.86	9.16
hayes-roth	5.92	9.26	8.03	10.3	8.09	8.58	4.57	7.82	5.92	9.55	6.86	7.24
	3.43	5.99	5.21	6.48	5.45	5.44	2.37	4.98	3.56	5.76	4.52	4.61
heart-cleveland	32.34	32.18	31.56	32.01	32.1	31.78	31.08	30.46	30.52	30.2	31	31.05
	19.01	19.59	18.77	19.27	19.53	19.35	16.28	16.73	16.64	16.38	17.69	17.68
heart-hungarian	17.72	17.95	18.06	17.68	18.68	17.26	15.66	15.94	16.59	15.6	16.65	16.44
	9.05	9.54	9.56	9.41	10.05	9.19	7.06	7.67	7.92	7.52	8.34	8.12
heart-switzerland	17.46	17.32	17.33	17.45	17.62	17.52	17.16	17.5	17.15	17.44	17.58	17.24
	9.94	10.18	10.02	10.2	10.31	10.23	9.04	9.31	8.9	9.19	9.78	9.66
heart-va	29.78	29.76	29.87	29.57	29.55	29.72	29.61	30.17	29.46	29.33	29.59	29.76
	17.39	17.41	17.36	17.5	17.44	17.49	15.93	16.11	16.02	16.16	16.35	16.34
hepatitis	8.91	9.79	9.41	9.57	9.48	9.05	8.82	9.19	8.89	9.06	9.04	8.96
	4.91	5.54	5.26	5.5	5.45	5.18	4.71	5.11	4.81	5.04	4.92	4.88
hill-valley	293.58	272.38	281	268.79	281.38	273.96	290.39	264.8	274.21	261.01	271.99	267.73
	135.21	143.5	144.06	137.19	145	138.52	132.08	141.33	142.91	131.17	142.78	137.4
horse-colic	18.23	20.99	19.67	20.73	22.68	22.33	16.51	19.16	18.7	20.2	21.22	22.24
	10.34	11.9	11.27	11.99	12.96	12.69	8.78	10.51	10.31	11.22	11.82	12.32
ilpd-indian-liver	48.37	48.88	49.08	50.59	48.99	49.22	46.68	46.75	46.17	47.11	46.68	47.47
	23.29	23.55	23.93	24.73	24.41	24.09	20.95	20.99	21.37	21.25	22.14	22.45
image-segmentation	380.59	466.36	424.88	623.46	457.6	468.05	298.42	393.75	338.4	588.04	378.66	392.93
	295.25	377.07	348.3	520.25	375.6	398.97	227.28	315.87	270.57	490.47	315.18	339.2
ionosphere	13.06	14.02	14.4	14.62	14.84	13.84	10.89	12.21	12.45	12.83	13.34	12.7
	7.97	9.19	9.42	9.32	9.71	8.95	6.4	8	8.19	8.4	8.69	8
iris	2.02	2.11	1.77	2.02	2.77	1.55	1.95	1.52	1.59	1.39	2.28	1.54
	1.08	1.33	1.13	1.42	2.02	0.88	0.84	0.78	0.86	0.81	1.46	0.88
led-display	79.9	84.24	80.89	90.26	78.53	79.14	78.8	83.67	80.07	90.53	77.87	78.75
	38.74	45.57	40.56	55.39	38.18	38.21	28.95	35.1	31.03	49.77	26.71	29.18
lenses	1.93	1.85	1.77	2.06	2.13	1.96	1.64	1.8	1.94	1.57	1.9	1.79
	1.32	1.28	1.17	1.31	1.39	1.33	1.02	1.15	1.17	1.05	1.2	1.14
letter	875.1	1169.82	1122.19	1298.45	1182.43	1040.52	684.66	988.71	890.24	1159.74	940.64	816.4
	764.88	1047.64	1001.99	1159.21	1055.78	932.48	594	890.77	802.66	1044.75	852.52	743.86
libras	39.03	34	39.06	36.55	38.12	37.04	30.97	27.25	31.19	30.93	29.77	28.47
	29.95	27.67	31.79	29.51	30.76	29.78	23.66	22.48	25.89	25.5	24.2	23.26
low-res-spect	21.91	21.87	23.23	26.01	25.24	23.35	20.2	20.31	21.19	23.63	21.42	19.92
	14.56	14.63	16.17	18.25	18.37	16.53	12.33	12.7	13.87	16.04	14.45	13.34
lung-cancer	4.26	4.17	4.33	4.34	4.44	4.39	3.98	4.31	4.06	4.23	4.2	4.26
	2.41	2.45	2.38	2.48	2.55	2.51	2.14	2.45	2.13	2.43	2.43	2.39
lymphography	29.68	29.16	29.39	28.59	29.28	30	30.62	29.47	30.51	29.1	29.72	29.84
	6.14	7.17	6.35	7.45	7.16	6.57	4.95	6.21	5.02	6.48	6.17	5.89
magic	966.3	1008.49	1008.6	1004.6	996.78	976.48	898	916.77	941.86	896.96	920.04	910.56
	505.97	533.54	537.45	534.69	542.88	522.07	448	448.36	481.86	437.62	486.41	474.26
mammographic	54.54	53.46	57.6	52.97	56.38	57.43	52.55	50.14	52.68	50.64	52.91	53.6
	23.19	21.7	24.86	21.59	23.8	24.96	14.66	15.31	16.96	17.48	16.02	16.37
miniboone	4121.21	3859.11	4216.63	3803.82	4551.71	4175.43	3858.53	3504.21	3965.63	3479.97	4206.87	3913.31
	2422.28	2162.95	2504.94	2050.18	2765.54	2493.98	2254.23	1914.7	2351.13	1853.21	2542.82	2335.05
molec-biol-promoter	9.42	10.33	9.78	10.49	11.02	9.94	8.33	9.79	9.17	9.58	10.18	9.34
	5.6	5.9	5.76	6.01	6.1	5.79	5.11	5.66	5.46	5.6	5.87	5.53
molec-biol-splice	181.66	290.79	213.17	297.37	306.32	244.77	145.8	261.31	180.77	267.25	269.7	214.22
	138.02	201.95	159.45	205.03	212.57	177.08	109.67	182.44	135.65	187.34	189.93	154.95
monks-1	184.7	188.87	190.15	193.74	190.17	189.89	179.06	181.61	184.26	191.03	188.55	182.31
	52.93	87.64	69.57	80.62	77.94	75.1	47.2	75.36	67.2	83.85	68.68	66.87
monks-2	153.7	157.68	155.9	162.69	163.26	160.78	148.77	150.26	151.06	154.24	154.44	154.19
	30.91	44.29	38.65	54.25	51.21	47.28	16.71	26.01	23.34	35.95	33.11	30.23
monks-3	194.02	172.46	188.45	184.22	188.32	192.86	200.1	169.54	186.25	188.42	181.59	190.13
	57.03	73.83	61.84	74.99	76.46	74.71	41.86	66.7	57.22	63.91	59.58	66.64
mushroom	3.18	6.41	3.36	27.9	9.02	7.78	2.21	4.61	2.23	22.76	9.97	4.58
	2.96	6.01	3.19	26.48	8.51	7.39	2.11	4.41	2.16	21.69	9.63	4.32
musk-1	36.02	37.26	39.74	38.63	41.52	38.78	30.47	32.76	34.15	34.71	35.13	34.42
	21.41	22.39	23.37	23.26	24.97	22.56	17.96	19.98	20.56	21.08	21.42	20.02
musk-2	115.57	146.03	149.62	159.35	175.74	157.47	74.74	114.79	115.99	122.98	125.67	120.31
	74.39	94.63	96.47	104.31	117.35	103.39	48.23	70.91	72.46	75.96	82.9	78.09
nursery	2030.12	1962.02	2014.15	1920.23	2004.34	2021.52	2058.12	1985.2	2046.31	1939.8	2050.82	2058
	161.98	238.37	178.16	324.16	198.46	171.28	132.12	209.75	140.91	314.17	150.08	132.66

(*continued on next page*)

Table 8 (*continued*).

Datasets	RaF Bias Variance	MPRaF-T Bias Variance	MPRaF-P Bias Variance	MPRaF-N Bias Variance	RaF-PCA Bias Variance	RaF-LDA Bias Variance	DRaF Bias Variance	MPDRaF-T* Bias Variance	MPDRaF-P* Bias Variance	MPDRaF-N* Bias Variance	DRaF-PCA* Bias Variance	DRaF-LDA* Bias Variance
OM_nucleus_4d	81.66	74.48	76.05	72.5	78.9	74.33	76.11	68.82	71.97	65.53	74.18	68
	42.31	40.62	41.99	37.79	44.34	42.02	38.87	37.36	39.42	33.5	41.79	37.88
OM_states_2f	34.01	34.28	34.58	35.49	37.72	32.94	31.06	30.45	31.41	31.39	33.8	29.99
	19.83	19.9	20.75	21.12	23.55	20.02	17.22	17.43	18.2	18.1	20.25	17.49
OT_nucleus_2f	74.58	72.35	73.19	71.7	73.64	69.96	68.6	66.13	68.06	66.72	68.15	64.49
	40.36	40.87	41.87	40.8	41.99	39.73	36.25	37.3	38.51	37.36	39.01	35.9
OT_states_5b	39.31	37.43	39.03	40.35	42.03	37.07	34.83	31.38	34.19	33.6	35.96	31.24
	23.74	23.71	24.49	25.67	27.71	24.22	20.25	19.51	21.27	20.76	23.37	20.16
optical	347.14	471.68	351.36	932.06	525.93	854.82	293.25	424.12	301.73	941.64	473.15	746.27
	311.63	429.48	317.48	724.69	482.75	698.24	265.14	391.18	272.43	729.29	443.37	643.02
ozone	30.14	30.46	30.64	29.86	35	33.74	28.36	26.49	27.92	24.97	30.81	30.67
	15	16.01	15.45	15.3	19.46	18.5	13.23	11.87	13.25	10.05	15.93	15.73
page-blocks	61.43	65.49	62.18	71.87	67.36	65.3	54.61	56.4	55.72	65.77	58.29	56.73
	34.01	36.47	35.83	42.22	39.94	38.53	24.99	27.94	27.59	36.35	30.5	29.61
parkinsons	9.43	9.15	9.53	9.47	10.49	9.77	7.89	7.72	8.06	8.14	8.98	8.24
	5.16	5.53	5.5	5.56	6.1	6.06	4.3	4.73	4.78	4.91	5.11	4.88
pendigits	432.84	349.16	411.69	461.57	442.92	392.22	371.49	296.03	353.34	415.33	390.87	340.92
	334.57	280.17	325.47	379.57	375	322.83	281.79	233.79	278.04	338.84	328.11	276.92
pima	62.07	63.41	63.57	64.1	64.12	63	60.56	60.16	61.79	59.96	62.36	61.22
	30.1	31.52	31.52	31.97	31.71	31.04	27.11	27.75	29.4	28.04	29.64	28.43
pittsburg-bridges-MATERIAL	4.32	3.93	4.51	4	4.56	4.33	3.65	3.28	3.64	3.27	3.69	3.34
	2.45	2.53	2.76	2.51	2.96	2.71	1.56	1.71	1.58	1.7	2.03	1.62
pittsburg-bridges-REL-L	9.87	9.77	9.89	9.77	10.05	10.19	9.04	8.99	9.16	8.98	9.28	9.05
	5.66	5.84	5.88	5.88	5.92	6.01	4.78	4.92	4.75	5	5.09	4.96
pittsburg-bridges-SPAN	9.73	9.39	9.7	9.57	9.61	9.55	9.36	8.72	9.08	8.87	9.26	9.19
	5.02	4.94	5	5.26	5.25	5.11	3.85	3.88	3.9	3.98	4.27	4.19
pittsburg-bridges-T-OR-D	3.8	4.23	3.76	3.95	4.11	4.08	3.13	3.13	3.18	3.29	3.6	3.51
	1.89	2.16	1.87	2	2.12	2.03	1.18	1.05	1.19	1.24	1.51	1.45
pittsburg-bridges-TYPE	11.06	11.16	11.43	11.38	11.39	11.44	10.23	9.92	10.1	10.34	10.45	10.18
	6.52	7.2	6.83	7.13	7.19	7.09	4.72	5.46	5.01	5.61	5.67	5.47
planning	18.94	18.72	19.12	18.83	19.18	18.78	18.43	17.87	17.96	16.92	18.36	18.3
	8.34	8.66	8.61	8.58	8.95	8.67	7.44	7.37	7.76	6.7	7.82	7.91
plant-margin	207.32	213.59	225.57	224.65	214.8	220.86	185.65	203.73	208.48	217.32	189.21	191.76
	165.7	168.02	175.83	174.65	169.32	173.42	150.92	162.44	166.6	170.34	153.6	156.81
plant-shape	208.39	200.15	218.05	213.26	207.39	210.35	187.89	186.74	199.96	201.49	181.49	179.02
	151.83	151.54	165.52	162.81	157.17	161.98	131.84	142.14	152.98	154.54	136.95	138.34
plant-texture	200.01	204.59	217.09	218.8	209.02	215.93	172.62	191.51	197.74	208.96	183.31	187.08
	161.71	165.22	173.28	173.36	167.88	172.22	142.61	156.98	161.7	167.84	150.72	155.16
post-operative	9.14	9.2	9.15	9.45	9.25	9.94	7.73	8.02	7.79	8.18	8.5	8.18
	3.58	3.53	3.47	3.78	3.54	3.92	1.69	1.94	1.81	2.07	2.28	2.12
primary-tumor	41.25	43.21	41.32	43.23	42.36	41.73	38.62	40.04	38.99	40.65	39.66	39.88
	26.24	28.4	26.7	29.11	27.75	27.34	20.98	23.19	21.99	25.14	23.35	24.13
ringnorm	256.67	306.79	304.97	304.71	263.7	276.46	213.73	285.23	281	275.01	220.26	231.47
	175.88	168.89	170.48	169.11	191.62	198.7	141.68	163.36	161.3	159.62	160.21	167
seeds	6.82	5.48	6.61	6.06	7.12	5.76	5.84	5.11	5.38	5.35	6.1	5.2
	3.77	3.24	3.87	3.42	4.32	3.24	3.1	2.75	3.02	2.81	3.47	2.92
semeion	126.93	163.75	139.3	167.68	162.94	144.83	106.49	150.44	118.57	154.24	138.95	121.39
	108.94	135.69	118.51	138.09	134.91	123.66	91.81	126.4	102.45	129.21	118.36	106.29
soybean	85.7	125.43	86.86	169.31	145.14	168.43	65.71	118.51	66.27	167.24	129.05	160.1
	70.2	109.22	71.29	140.08	126.74	141.95	49.24	104.9	50.77	139.17	115.31	137.44
spambase	135.46	161.62	143.8	179.6	156.4	149.42	113.87	140.49	121.61	156.76	131.21	128.29
	83.45	104.31	90.36	117.42	101.55	95.58	66.39	87.83	73.1	99.73	82.8	80.36
spect	74.55	78.75	75.48	81.66	81.93	79.26	70.13	75.54	71.13	76.95	77.76	76.27
	35.82	37.59	36.46	37.47	39.29	36.74	28.16	29.38	28.01	29.5	32.29	32.7
spectf	37.38	44.39	42.58	28.7	50.73	60.26	33.26	39.24	36.48	23	45.36	47.13
	22.54	28.01	26.71	15.24	32.63	37.78	18.92	24.42	21.91	9.16	28.63	29.82
statlog-australian-credit	72.45	76.02	74.31	72.89	75.22	75.5	73.17	75.86	75.58	75.18	75.13	75.66
	35.72	36.79	36.61	35.72	36.67	36.65	35.08	36.52	36.82	35.68	35.9	36.08
statlog-german-credit	82.59	86.24	83.99	85.12	85.53	83.99	76.37	80.24	79.5	80.47	80.94	79.28
	43.05	44.83	43.79	43.73	44.69	43.93	37.2	38.65	39.35	38.63	40.84	39.73
statlog-heart	17.4	17.22	17.67	17.85	17.62	17	16.33	15.9	16.24	16.6	16.49	16.19
	9.81	9.82	10	10.02	9.98	9.37	8.18	8.39	8.55	8.77	9.02	8.69
statlog-image	42.92	53.07	46.48	67.83	51.13	42.32	30.38	41.77	34.76	53.36	36.73	30.74
	32.37	41.95	36.4	54.87	41.79	33.69	22.42	32.39	26.73	42.74	29.24	23.59
statlog-landsat	330.98	325.12	327.45	343.26	351.89	334.89	301.92	298.76	298.83	317.8	316.78	306.57
	215.27	205.78	210.92	213.63	232.29	215.5	191.15	186.25	188.09	193.7	205.19	194.98

(*continued on next page*)

Table 8 (*continued*).

Datasets	RaF Bias Variance	MPRaF-T Bias Variance	MPRaF-P Bias Variance	MPRaF-N Bias Variance	RaF-PCA Bias Variance	RaF-LDA Bias Variance	DRaF Bias Variance	MPDRaF-T* Bias Variance	MPDRaF-P* Bias Variance	MPDRaF-N* Bias Variance	DRaF-PCA* Bias Variance	DRaF-LDA* Bias Variance
statlog-shuttle	14.63	62.49	26.19	169.51	59.99	77.66	8.09	69.82	21.17	159.44	55.01	53.09
	10.99	51.74	21.32	145.12	54.77	70.31	6.06	58.72	16.2	134.38	51.13	48.18
statlog-vehicle	68.72	68.8	67.81	70.73	72.12	67.28	62.6	64.3	62.07	65.36	65.54	60.85
	41.53	43.94	43.43	45.73	48.4	44.34	35.74	39.18	38.16	41.03	42.64	39.28
steel-plates	158.94	168.25	167.32	176.17	174.42	169.94	143.81	157.85	150.39	163.29	156.3	156.1
	102.96	111.27	110.38	115.95	116.19	112.44	89.65	101.28	97.22	107.58	102.84	100.54
synthetic-control	24.33	20.63	24.89	28.59	27.24	21.6	18.64	16.33	19.11	22.57	20.27	17.68
	19.91	17.23	20.25	23.2	21.5	17.6	15.27	13.42	15.76	18.25	16.36	14.55
teaching	18.3	18.48	18.38	18.72	18.77	18.5	17.13	17.95	17.34	18.54	17.15	17.22
	9.98	10.03	10.09	10.11	10.23	9.88	7.15	7.57	7.47	8.44	7.54	7.61
thyroid	96.4	235.15	103.95	764.03	327.21	473.01	85.6	217.64	84.42	714.99	347.09	433.88
	64.68	152.4	71.55	587.65	277.09	396.42	54.73	137.61	53.7	558.06	307.19	369.07
tic-tac-toe	47.05	49.97	49.88	53.77	51	50.03	37.48	39.81	40.57	47.01	39.98	39.69
	33.66	35.23	35.05	36.53	35.73	35.22	27.83	29.77	30.07	33.41	29.71	29.61
titanic	119.26	120.25	119.76	122.17	118.52	118.64	118.31	119.18	118.84	121.15	118.62	117.76
	13.4	15.83	14.35	17.7	12.64	12.65	7	11.63	8.12	16.16	8.8	7.18
trains	0.75	0.69	0.75	0.73	0.83	0.83	0.59	0.71	0.55	0.75	0.62	0.69
	0.44	0.44	0.45	0.44	0.47	0.47	0.38	0.42	0.35	0.45	0.4	0.43
twonorm	322.13	174.14	179.14	175.13	196.7	174.59	300.72	154.18	163.55	152.77	173.41	156.68
	228.03	123.14	128.34	123.87	140.69	123.59	212.1	107.54	114.87	106.02	122.73	109.67
vertebral-column-2clases	18.23	17.96	18.07	18.48	19.07	17.83	17.34	16.3	16.55	16.32	17.53	16.7
	9.64	9.9	9.85	9.84	10.22	9.72	8.37	8.37	8.7	8.23	8.81	8.62
vertebral-column-3clases	18.24	19.38	18.97	19.38	19.65	18.88	16.69	17.36	17.24	17.18	18.4	16.97
	10.39	11.58	11.49	11.48	11.94	11.35	9	9.59	9.7	9.74	10.76	9.47
wall-following	53.4	263.94	147.78	279.8	217.02	205.71	34.78	209.91	116.49	228.6	161.01	150.81
	44.51	195.14	121.8	208.18	171.9	161.23	28.59	152.31	94.1	169.25	125.62	116.59
waveform	338.3	330.24	329.75	329.77	342.18	304.07	325.41	310.76	310.6	307.43	324.3	292.42
	200.61	195.75	195.75	196.45	207.55	177.82	185.88	180.54	181.45	179.29	192.39	166.3
waveform-noise	365.29	396.83	373.3	402.08	402.48	346.01	346.85	370.86	356.66	371.62	373.77	323.59
	229.31	250.02	234.66	254.27	259.66	215.75	212.51	231	220.16	232.58	237.8	199.23
wine	4.7	4.16	4.63	4.9	5.94	4.44	3.9	3.97	3.44	4.12	4.59	3.28
	3.7	3.32	3.72	3.85	4.53	3.6	3.03	3.04	2.72	3.2	3.55	2.66
wine-quality-red	170.47	172.33	170.37	172.22	170.12	169.33	152.43	159.31	152.86	160.16	150.89	148.68
	98.56	102.89	99.29	101.99	101.58	101.11	82.49	89.32	85.4	89.21	85.87	83.8
wine-quality-white	538.74	544.35	539.74	550.6	540.62	538.74	474.95	498.56	478.36	509.12	470.59	466.43
	323.98	333.7	327.45	333.24	333.04	330.1	268.98	290.93	274.29	295.78	274.59	268.83
yeast	171.29	178.95	172.73	179.09	173.81	173.4	164.8	172.82	165.84	173.92	166.39	165.68
	99.69	109.78	102.5	109.3	104.37	103.6	85.57	97.63	88.63	99.42	91.59	91.27
zoo	2.46	2.62	2.37	3.11	3.11	2.94	1.62	2.02	1.49	2.16	2.22	1.93
	2.11	2.35	2.03	2.65	2.78	2.65	1.37	1.68	1.26	1.85	2.01	1.72

Here, OM denotes oocytes_merluccius, OT denotes oocytes_trisopterus.

Table 9
Significant difference among the standard and double variants of the ensembles of decision trees based on the bias analysis.

Methods	Average rank	Average rank difference	Significance
(RaF, DRaF)	(7, 3.02)	3.98	Yes
(MPRaF-T, MPDRaF-T)	(8.52, 4.37)	4.15	Yes
(MPRaF-P, MPDRaF-P)	(7.96, 3.55)	4.41	Yes
(MPRaF-N, MPDRaF-N)	(9.73, 5.9)	3.83	Yes
(RaF-PCA, DRaF-PCA)	(10.03, 5.5)	4.53	Yes
(RaF-LDA, DRaF-LDA)	(8.42, 4.01)	4.41	Yes

$\chi_F^2 = 615.0719, F_F = 103.0950, q_{0.05} = 3.2680$. The two models are significantly different if the average ranks of the two models differ at least by the critical difference, $CD = 1.5149$.

Table 10
Significant difference among the standard and double variants of the ensembles of decision trees based on the variance analysis.

Methods	Average rank	Average rank difference	Significance
(RaF, DRaF)	(6.61, 1.93)	4.68	Yes
(MPRaF-T, MPDRaF-T)	(8.96, 4.03)	4.93	Yes
(MPRaF-P, MPDRaF-P)	(8.13, 3.36)	4.77	Yes
(MPRaF-N, MPDRaF-N)	(9.88, 5.64)	4.24	Yes
(RaF-PCA, DRaF-PCA)	(10.68, 5.64)	5.04	Yes
(RaF-LDA, DRaF-LDA)	(8.93, 4.2)	4.73	Yes

$\chi_F^2 = 809.8335, F_F = 186.4664, q_{0.05} = 3.2680$. The two models are significantly different if the average ranks of the two models differ at least by the critical difference, $CD = 1.5149$.

In this study, we consider $0-1$ loss function to analyze the performance of the models (Kohavi et al., 1996). For details of bias–variance analysis via $0-1$ loss, refer to Section 5 of the supplementary file. Let D and Y be spaces representing the input and output, respectively. Suppose $|D|$ represents the cardinality of D and $|Y|$ represents the cardinality of Y. Also, let $d \in D$ and $y \in Y$ be the element its label respectively. The conditional probability distribution of target f is $P(Y_F = y_F|d)$ where Y_F is the Y-valued random variable. Then for a single test data sample:

$$E(C) = \sum_d P(D)[(bias_d)^2 + \sigma_d^2 + variance_d], \tag{17}$$

where

$$(bias_d)^2 = \frac{1}{2}\sum_{y\in Y}[P(Y_F = y) - P(Y_H = y)]^2, \tag{18}$$

$$variance_d = \frac{1}{2}[1 - \sum_{y\in Y} P(Y_H = y)^2], \tag{19}$$

$$\sigma_d^2 = \frac{1}{2}[1 - \sum_{y\in Y} P(Y_H = y)^2]. \tag{20}$$

Here, $(bias_d)^2$ and $variance_d$ are calculated are each model and for each dataset. $(bias_d)^2$ is abbreviated as $bias_d$. Theoretically, the error should be decomposed into squared bias, variance and noise (also known as irreducible error). However, given the real-world tasks wherein the true underlying probability distribution is unknown, estimation of noise is difficult task. In commonly used approach, the noise is generally aggregated into bias and variance or the only bias term as the noise in invariant across the learning models for a given task and hence not a significant factor for the comparative analysis of the algorithms. Table 8 gives the bias–variance values for each model corresponding to the 121 datasets. In most of the cases the double variant ensembles of decision trees have the best bias–variance values compared to the standard ensembles of the decision trees.

We evaluate the bias–variance of the classification models via statistical tests. In this test, the lower value of bias/variance gets lower rank and vice versa. The analysis of the results for bias and variance are given in Tables 9 and 10, respectively. From the given tables, it is clear that the double variants of the random forest achieve lower average rank compared to the standard variants of random forest for both bias and variance performance. Hence, the proposed double variants of random forest show better bias–variance results compared to the standard variants of the random forest. Moreover, all the proposed variants of the double random forest are significantly better compared to the standard variants of the random forest.

9. Conclusion

In this paper, we propose two approaches for generating the double random forest models. In the first model, we propose oblique double random forest ensemble models and in the second approach, we propose rotation based double random forest ensemble models. In oblique double random forest models, the splitting hyperplane at each non-leaf node is generated via MPSVM. This leads to the incorporation of geometric structure and hence, leads to better generalization performance. As the decision tree grows, the problem of sample size may arise. Hence, we use Tikhonov regularization, axis parallel split regularization null space regularization for generating decision trees to full depth. In rotation based double random forest models, we used two transformations — principal component analysis and linear discriminant analysis, on randomly chosen feature subspace at each non-leaf node. Rotations on different random subspace features lead to more diverse decision tree ensembles and better generalization performance. Unlike standard random forest where the bootstrap aggregation is used at root node only, the proposed oblique and rotation double random forest use bootstrap aggregation at each non-terminal node for choosing the best split and then the original samples are sent down the decision trees. The proposed double variants of the ensemble of decision trees results in bigger trees compared to the standard variants of the ensemble of decision trees. Experimental results and the statistical analysis show the efficacy of the proposed oblique and rotation double random forest ensemble models over standard baseline classifiers. Besides classification, we will expand this work to regression and times series forecasting problems in the future. Moreover, one can also perform benchmarking of the variants of the standard random forest, variants of double random forest and XGBoost to evaluate their performance on a common platform which can help in choosing the best model.

Declaration of competing interest

The authors declare that they have no known competing financial interests or personal relationships that could have appeared to influence the work reported in this paper.

Acknowledgments

This work is supported by Science and Engineering Research Board (SERB), Government of India under Ramanujan Fellowship Scheme, Grant No. SB/S2/RJN-001/2016, and Department of Science and Technology under Interdisciplinary Cyber Physical Systems (ICPS) Scheme grant no. DST/ICPS/CPS-Individual/2018/276. We gratefully acknowledge the Indian Institute of Technology Indore for providing facilities and support.

Appendix A. Supplementary data

Supplementary material related to this article can be found online at https://doi.org/10.1016/j.neunet.2022.06.012.

References

Banfield, R. E., Hall, L. O., Bowyer, K. W., & Kegelmeyer, W. P. (2006). A comparison of decision tree ensemble creation techniques. *IEEE Transactions on Pattern Analysis and Machine Intelligence*, *29*, 173–180.

Bottou, L., Cortes, C., Denker, J. S., Drucker, H., Guyon, I., Jackel, L. D., et al. (1994). Comparison of classifier methods: A case study in handwritten digit recognition. In *Proceedings of the 12th IAPR international conference on pattern recognition, Vol. 3-conference C: signal processing (Cat. No. 94CH3440-5)*: *Vol. 2*, (pp. 77–82). IEEE.

Boulesteix, A. -L., Janitza, S., Kruppa, J., & König, I. R. (2012). Overview of random forest methodology and practical guidance with emphasis on computational biology and bioinformatics. *Wiley Interdisciplinary Reviews: Data Mining and Knowledge Discovery*, *2*, 493–507.

Breiman, L. (1996a). *Bias, variance, and arcing classifiers*: *Tech. Rep. 460*, Berkeley: Statistics Department, University of California.

Breiman, L. (1996b). Bagging predictors. *Machine Learning*, *24*, 123–140.

Breiman, L. (2001). Random forests. *Machine Learning*, *45*, 5–32.

Breiman, L., Friedman, J., Stone, C. J., & Olshen, R. A. (1984). *Classification and regression trees*. CRC Press.

Cantu-Paz, E., & Kamath, C. (2003). Inducing oblique decision trees with evolutionary algorithms. *IEEE Transactions on Evolutionary Computation*, *7*, 54–68.

Cha, S. -H., & Tappert, C. C. (2009). A genetic algorithm for constructing compact binary decision trees. *Journal of Pattern Recognition Research*, *4*, 1–13.

Chen, L. -F., Liao, H. -Y. M., Ko, M. -T., Lin, J. -C., & Yu, G. -J. (2000). A new LDA-based face recognition system which can solve the small sample size problem. *Pattern Recognition*, *33*, 1713–1726.

Chu, C., Kim, S. K., Lin, Y., Yu, Y., Bradski, G., Ng, A. Y., et al. (2007). Map-reduce for machine learning on multicore. *Advances in Neural Information Processing Systems*, *19*, 281.

Cortes, C., & Vapnik, V. (1995). Support-vector networks. *Machine Learning*, *20*, 273–297.

Demšar, J. (2006). Statistical comparisons of classifiers over multiple data sets. *Journal of Machine Learning Research*, *7*, 1–30.

Dietterich, T. G. (2000). Ensemble methods in machine learning. In *International workshop on multiple classifier systems* (pp. 1–15). Springer.

Dietterich, T. G., & Bakiri, G. (1994). Solving multiclass learning problems via error-correcting output codes. *Journal of Artificial Intelligence Research*, *2*, 263–286.

Dua, D., & Graff, C. (2017). *UCI Machine Learning Repository*. University of California, Irvine, School of Information and Computer Sciences, URL: http://archive.ics.uci.edu/ml.

Dwork, C. (2008). Differential privacy: A survey of results. In *International conference on theory and applications of models of computation* (pp. 1–19). Springer.

Fernández, R. R., de Diego, I. M., Aceña, V., Fernández-Isabel, A., & Moguerza, J. M. (2020). Random forest explainability using counterfactual sets. *Information Fusion*, *63*, 196–207.

Fernández-Delgado, M., Cernadas, E., Barro, S., & Amorim, D. (2014). Do we need hundreds of classifiers to solve real world classification problems? *Journal of Machine Learning Research*, *15*, 3133–3181.

Fletcher, S., & Islam, M. Z. (2017). Differentially private random decision forests using smooth sensitivity. *Expert Systems with Applications*, *78*, 16–31.

Freeman, E. A., Moisen, G. G., Coulston, J. W., & Wilson, B. T. (2016). Random forests and stochastic gradient boosting for predicting tree canopy cover: Comparing tuning processes and model performance. *Canadian Journal of Forest Research*, *46*, 323–339.

Friedman, J. H. (1997). On bias, variance, 0/1—loss, and the curse-of-dimensionality. *Data Mining and Knowledge Discovery*, *1*, 55–77.

Ganaie, M. A., Ghosh, S., Mendola, N., Tanveer, M., & Jalan, S. (2020). Identification of chimera using machine learning. *Chaos. An Interdisciplinary Journal of Nonlinear Science*, *30*, Article 063128.

Ganaie, M. A., Tanveer, M., & Suganthan, P. N. (2020). Oblique decision tree ensemble via twin bounded SVM. *Expert Systems with Applications*, *143*, Article 113072.

Geman, S., Bienenstock, E., & Doursat, R. (1992). Neural networks and the bias/variance dilemma. *Neural Computation*, *4*, 1–58.

Geurts, P., Ernst, D., & Wehenkel, L. (2006). Extremely randomized trees. *Machine Learning*, *63*, 3–42.

Goerss, J. S. (2000). Tropical cyclone track forecasts using an ensemble of dynamical models. *Monthly Weather Review*, *128*, 1187–1193.

González-Rufino, E., Carrión, P., Cernadas, E., Fernández-Delgado, M., & Domínguez-Petit, R. (2013). Exhaustive comparison of colour texture features and classification methods to discriminate cells categories in histological images of fish ovary. *Pattern Recognition*, *46*, 2391–2407.

Guan, Z., Sun, X., Shi, L., Wu, L., & Du, X. (2020). A differentially private greedy decision forest classification algorithm with high utility. *Computers & Security*, *96*, Article 101930.

Han, S., & Kim, H. (2019). On the optimal size of candidate feature set in random forest. *Applied Sciences*, *9*, 898.

Han, S., Kim, H., & Lee, Y. -S. (2020). Double random forest. *Machine Learning*, *109*, 1569–1586.

Hernández-Lobato, D., MartíNez-MuñOz, G., & Suárez, A. (2013). How large should ensembles of classifiers be? *Pattern Recognition*, *46*, 1323–1336.

Ho, T. K. (1998). The random subspace method for constructing decision forests. *IEEE Transactions on Pattern Analysis and Machine Intelligence*, *20*, 832–844.

Hothorn, T., Leisch, F., Zeileis, A., & Hornik, K. (2005). The design and analysis of benchmark experiments. *Journal of Computational and Graphical Statistics*, *14*, 675–699.

Huang, B. F. F., & Boutros, P. C. (2016). The parameter sensitivity of random forests. *BMC Bioinformatics*, *17*, 331.

James, G. M. (2003). Variance and bias for general loss functions. *Machine Learning*, *51*, 115–135.

Jiang, X. (2011). Linear subspace learning-based dimensionality reduction. *IEEE Signal Processing Magazine*, *28*, 16–26.

Jiang, H., Deng, Y., Chen, H. -S., Tao, L., Sha, Q., Chen, J., et al. (2004). Joint analysis of two microarray gene-expression data sets to select lung adenocarcinoma marker genes. *BMC Bioinformatics*, *5*, 81.

Katuwal, R., Suganthan, P. N., & Zhang, L. (2020). Heterogeneous oblique random forest. *Pattern Recognition*, *99*, Article 107078.

Klambauer, G., Unterthiner, T., Mayr, A., & Hochreiter, S. (2017). Self-normalizing neural networks. *Advances in Neural Information Processing Systems*, *30*.

Knerr, S., Personnaz, L., & Dreyfus, G. (1990). Single-layer learning revisited: A stepwise procedure for building and training a neural network. In *Neurocomputing* (pp. 41–50). Springer.

Kohavi, R., Wolpert, D. H., et al. (1996). Bias plus variance decomposition for zero-one loss functions. In *ICML: Vol. 96*, (pp. 275–283).

Kong, E. B., & Dietterich, T. G. (1995). Error-correcting output coding corrects bias and variance. In *Machine learning proceedings 1995* (pp. 313–321). Elsevier.

Kreßner, D. (2004). Numerical methods and software for general and structured eigenvalue problems.

Lin, Y., & Jeon, Y. (2006). Random forests and adaptive nearest neighbors. *Journal of the American Statistical Association*, *101*, 578–590.

Lulli, A., Oneto, L., & Anguita, D. (2017a). Crack random forest for arbitrary large datasets. In *2017 IEEE international conference on big data* (pp. 706–715). IEEE.

Lulli, A., Oneto, L., & Anguita, D. (2017b). ReForeSt: Random forests in apache spark. In *International conference on artificial neural networks* (pp. 331–339). Springer.

Lulli, A., Oneto, L., & Anguita, D. (2019). Mining big data with random forests. *Cognitive Computation*, *11*, 294–316.

Mangasarian, O. L., & Wild, E. W. (2005). Multisurface proximal support vector machine classification via generalized eigenvalues. *IEEE Transactions on Pattern Analysis and Machine Intelligence*, *28*, 69–74.

Manwani, N., & Sastry, P. S. (2011). Geometric decision tree. *IEEE Transactions on Systems, Man and Cybernetics, Part B (Cybernetics)*, *42*, 181–192.

Margineantu, D. D., & Dietterich, T. G. (1997). Pruning adaptive boosting. *Vol. 97*, In *ICML* (pp. 211–218). Citeseer.

Marroquin, J., Mitter, S., & Poggio, T. (1987). Probabilistic solution of ill-posed problems in computational vision. *Journal of the American Statistical Association*, *82*, 76–89.

Martínez-Muñoz, G., & Suárez, A. (2010). Out-of-bag estimation of the optimal sample size in bagging. *Pattern Recognition*, *43*, 143–152.

Maudes, J., Rodríguez, J. J., García-Osorio, C., & García-Pedrajas, N. (2012). Random feature weights for decision tree ensemble construction. *Information Fusion*, *13*, 20–30.

Menze, B. H., Kelm, B. M., Masuch, R., Himmelreich, U., Bachert, P., Petrich, W., et al. (2009). A comparison of random forest and its Gini importance with standard chemometric methods for the feature selection and classification of spectral data. *BMC Bioinformatics*, *10*, 213.

Menze, B. H., Petrich, W., & Hamprecht, F. A. (2007). Multivariate feature selection and hierarchical classification for infrared spectroscopy: Serum-based detection of bovine spongiform encephalopathy. *Analytical and Bioanalytical Chemistry*, *387*, 1801–1807.

Murthy, S. K., Kasif, S., Salzberg, S., & Beigel, R. (1993). OC1: A randomized algorithm for building oblique decision trees. In *Proceedings of AAAI*: *Vol. 93*, (pp. 322–327). Citeseer.

Murthy, K. V. S., & Salzberg, S. L. (1995). *On growing better decision trees from data* (Ph.D. thesis), Citeseer.

Nemenyi, P. (1962). Distribution-free multiple comparisons. In *Biometrics*: *Vol. 18*, (p. 263). International Biometric Soc 1441 I ST, NW, Suite 700, Washington, DC 20005-2210.

Oshiro, T. M., Perez, P. S., & Baranauskas, J. A. (2012). How many trees in a random forest? In *International workshop on machine learning and data mining in pattern recognition* (pp. 154–168). Springer.

Pal, M., & Parija, S. (2021). Prediction of heart diseases using random forest. *Journal of Physics: Conference Series*, *1817*, Article 012009.

Pangilinan, J. M., & Janssens, G. K. (2011). Pareto-optimality of oblique decision trees from evolutionary algorithms. *Journal of Global Optimization*, *51*, 301–311.

Patil, A., & Singh, S. (2014). Differential private random forest. In *2014 international conference on advances in computing, communications and informatics* (pp. 2623–2630). IEEE.

Pedrycz, W., & Sosnowski, Z. A. (2005). Genetically optimized fuzzy decision trees. *IEEE Transactions on Systems, Man and Cybernetics, Part B (Cybernetics)*, *35*, 633–641.

Platt, J., Cristianini, N., & Shawe-Taylor, J. (1999). Large margin DAGs for multiclass classification. *Advances in Neural Information Processing Systems*, *12*, 547–553.

Probst, P., & Boulesteix, A. -L. (2017). To tune or not to tune the number of trees in random forest. *Journal of Machine Learning Research*, *18*, 6673–6690.

Rodriguez, J. J., Kuncheva, L. I., & Alonso, C. J. (2006). Rotation forest: A new classifier ensemble method. *IEEE Transactions on Pattern Analysis and Machine Intelligence*, *28*, 1619–1630.

Rokach, L. (2016). Decision forest: Twenty years of research. *Information Fusion*, *27*, 111–125.

Sagi, O., & Rokach, L. (2020). Explainable decision forest: Transforming a decision forest into an interpretable tree. *Information Fusion*, *61*, 124–138.

Shao, Y. -H., Zhang, C. -H., Wang, X. -B., & Deng, N. -Y. (2011). Improvements on twin support vector machines. *IEEE Transactions on Neural Networks*, *22*, 962–968.

Shen, K. -Q., Ong, C. -J., Li, X. -P., Hui, Z., & Wilder-Smith, E. P. (2007). A feature selection method for multilevel mental fatigue EEG classification. *IEEE Transactions on Biomedical Engineering*, *54*, 1231–1237.

Wang, X. -Z., & Dong, C. -R. (2008). Improving generalization of fuzzy IF–THEN rules by maximizing fuzzy entropy. *IEEE Transactions on Fuzzy Systems*, *17*, 556–567.

Wang, X. -Z., Zhai, J. -H., & Lu, S. -X. (2008). Induction of multiple fuzzy decision trees based on rough set technique. *Information Sciences*, *178*, 3188–3202.

Wiering, M. A., & Van Hasselt, H. (2008). Ensemble algorithms in reinforcement learning. *IEEE Transactions on Systems, Man and Cybernetics, Part B (Cybernetics)*, *38*, 930–936.

Xin, B., Yang, W., Wang, S., & Huang, L. (2019). Differentially private greedy decision forest. In *ICASSP 2019-2019 IEEE international conference on acoustics, speech and signal processing* (pp. 2672–2676). IEEE.

Zhang, L., Ren, Y., & Suganthan, P. N. (2014). Towards generating random forests via extremely randomized trees. In *2014 international joint conference on neural networks* (pp. 2645–2652). IEEE.

Zhang, L., & Suganthan, P. N. (2014a). Oblique decision tree ensemble via multisurface proximal support vector machine. *IEEE Transactions on Cybernetics*, *45*, 2165–2176.

Zhang, L., & Suganthan, P. N. (2014b). Random forests with ensemble of feature spaces. *Pattern Recognition*, *47*, 3429–3437.

Zhang, L., & Suganthan, P. N. (2017). Benchmarking ensemble classifiers with novel co-trained kernel ridge regression and random vector functional link ensembles [research frontier]. *IEEE Computational Intelligence Magazine*, *12*, 61–72.

Zhang, C. -X., & Zhang, J. -S. (2008). RotBoost: A technique for combining rotation forest and AdaBoost. *Pattern Recognition Letters*, *29*, 1524–1536.

Zhang, L., Zhou, W. -D., Su, T. -T., & Jiao, L. -C. (2007). Decision tree support vector machine. *International Journal on Artificial Intelligence Tools*, *16*, 1–15.

Zhou, Z. -H., Roli, F., Kittler, J., et al. (2013). Multiple classifier systems. In *Proc. 2013 11th int. workshop mult. classifier syst.* (p. 24). Springer.